ORIGINAL RESEARCH

Protein Kinase D1 Regulates Cardiac Hypertrophy, Potassium Channel Remodeling, and Arrhythmias in Heart Failure

Julie Bossuyt [iD], DVM, PhD; Johanna M. Borst [iD], MD; Marie Verberckmoes, MS; Logan R. J. Bailey [iD], BS; Donald M. Bers [iD], PhD; Bence Hegyi [iD], MD, PhD

BACKGROUND: Structural and electrophysiological remodeling characterize heart failure (HF) enhancing arrhythmias. PKD1 (protein kinase D1) is upregulated in HF and mediates pathological hypertrophic signaling, but its role in K+ channel remodeling and arrhythmogenesis in HF is unknown.

METHODS AND RESULTS: We performed echocardiography, electrophysiology, and expression analysis in wild-type and PKD1 cardiomyocyte-specific knockout (cKO) mice following transverse aortic constriction (TAC). PKD1-cKO mice exhibited significantly less cardiac hypertrophy post-TAC and were protected from early decline in cardiac contractile function (3 weeks post-TAC) but not the progression to HF at 7 weeks post-TAC. Wild-type mice exhibited ventricular action potential duration prolongation at 8 weeks post-TAC, which was attenuated in PKD1-cKO, consistent with larger K+ currents via the transient outward current, sustained current, inward rectifier K+ current, and rapid delayed rectifier K+ current and increased expression of corresponding K+ channels. Conversely, reduction of slowly inactivating K+ current was independent of PKD1 in HF. Acute PKD inhibition slightly increased transient outward current in TAC and sham wild-type myocytes but did not alter other K+ currents. Sham PKD1-cKO versus wild-type also exhibited larger transient outward current and faster early action potential repolarization. Tachypacing-induced action potential duration alternans in TAC animals was increased and independent of PKD1, but diastolic arrhythmogenic activities were reduced in PKD1-cKO.

CONCLUSIONS: Our data indicate an important role for PKD1 in the HF-related hypertrophic response and K+ channel downregulation. Therefore, PKD1 inhibition may represent a therapeutic strategy to reduce hypertrophy and arrhythmias; however, PKD1 inhibition may not prevent disease progression and reduced contractility in HF.

Key Words: action potential ■ cardiac arrhythmia ■ heart failure ■ hypertrophic signaling ■ potassium channels

PKD (protein kinase D) is a serine/threonine kinase that regulates numerous cell functions in a spatio-temporal manner via gene transcription, intracellular trafficking, and phosphorylation of target proteins.[1–4] Moreover, upregulation of PKD1 (the predominant cardiac isoform) is associated with pathological cardiac hypertrophy.[5–9] Enhanced PKD1 signaling is known to induce so-called fetal gene reactivation leading to pronounced structural and functional remodeling upon sustained cardiac stress.[10,11] Cardiac-specific deletion of PKD1 has been shown to prevent cardiac hypertrophy in several cardiac stress models including pressure overload via transverse aortic constriction (TAC) and chronic exposure to angiotensin II or isoproterenol.[7] It is still debated whether pathological cardiac hypertrophy (different from physiological cardiac hypertrophy that develops upon physical exercise) is ever compensatory or whether it is detrimental from the onset.[12–14] However, sustained

JAHA is available at: www.ahajournals.org/journal/jaha

CLINICAL PERSPECTIVE

What Is New?

- Cardiomyocyte-specific deletion of PKD1 (protein kinase D1) attenuated cardiac hypertrophy but did not prevent chronic heart failure (HF) development induced by pressure overload.
- PKD1 significantly contributed to action potential duration prolongation and remodeling of K+ channels in HF, predominantly via downregulating K+ channel gene transcription.
- PKD1 knockout was protective against delayed afterdepolarizations but did not affect the magnitude of cardiac alternans in HF.

What Are the Clinical Implications?

- PKD1 is a potential therapeutic target and PKD1 inhibition may have important antiarrhythmic properties in HF.
- Prevention of cardiac hypertrophy does not directly translate into protection against HF.
- There is a mismatch between cardiac hypertrophy—K+ channel downregulation—prolongation of action potential duration and disease development and progression.

Nonstandard Abbreviations and Acronyms

APD	action potential duration
CaMKII	Ca^{2+}/calmodulin-dependent protein kinase II
cKO	cardiomyocyte-specific knockout
CREB	cAMP response element binding protein
DAD	delayed afterpolarization
I_{K1}	inward rectifier K+ current
I_{Kr}	rapid delayed rectifier K+ current
$I_{K,slow}$	slowly inactivating K+ current
I_{to}	transient outward K+ current
I_{sus}	sustained K+ current
PKD	protein kinase D
SR	sarcoplasmic reticulum
TAC	transverse aortic constriction
WT	wild type

pathological stresses and hypertrophy exert unambiguously deleterious effects on cardiac metabolism and energetics, and may contribute to disease progression towards heart failure (HF). Moreover, inhibition of cardiac hypertrophy has been suggested as a potential therapeutic strategy to preserve cardiac function.[15–18]

Besides contractile and energetic deficits, cardiac hypertrophy and HF are also associated with increased risk of cardiac arrhythmias.[19] K+ channel remodeling in cardiac hypertrophy and HF significantly contributes to action potential duration (APD) prolongation leading to long QT interval on ECG, a known risk factor for arrhythmias.[20] Decreased inward rectifier K+ current (I_{K1}) and transient outward K+ current (I_{to}) have been consistently observed in hypertrophy and HF in both animal and human studies.[20–24] One study in diet-induced obesity found association between up-regulation of PKD and downregulation of CREB (cAMP response element binding protein) leading to downregulation of multiple K+ channels.[25] However, the exact role of PKD1 signaling in the regulation of K+ currents in healthy and diseased hearts remains unclear.

Previous studies of PKD1 focused on the early cardiac remodeling and the hypertrophy phase (3 to 4 weeks post-TAC),[7,26] but to date no information is available on how PKD1 affects the chronic HF-related outcomes (7 to 8 weeks post-TAC). In this study, we aimed to investigate the role of PKD1 in cardiac hypertrophy, contractile function, K+ channel downregulation, and arrhythmogenic electrophysiological remodeling in a murine model of TAC-induced congestive HF.

METHODS

The data that support the findings of this study are available from the corresponding authors upon reasonable request.

All animal handling and laboratory procedures were in accordance with the approved protocols (#21064 and #21572) of the Institutional Animal Care and Use Committee at University of California, Davis conforming to the *Guide for the Care and Use of Laboratory Animals* published by the National Institutes of Health (8th edition, 2011).

Detailed description of the materials and methods is available in Data S1.

Animal Model and Cardiomyocyte Isolation

C57BL/6J mice with cardiomyocyte-specific knockout (cKO) of PKD1 was obtained by crossing PKD1$^{loxP/loxP}$ mice (Jackson Laboratory, stock No.: 014181) with PKD1$^{loxP/loxP; \alpha-MHC-Cre}$ mice as described.[7]

PKD1 cKO (n=13) and wild-type (WT) littermate (n=16) 10-week-old mice were subjected to pressure overload by TAC as described.[27] Briefly, after deep anesthesia was induced with 2% to 4% isoflurane inhalation in 100% oxygen, a small incision was made into the thoracic cavity in the second intercostal space. The transverse aorta was ligated with suture tied against a 28-gauge wire. Successful constriction of the aorta was confirmed by measuring the pressure gradient and observation of diminished left carotid artery perfusion.

A sham procedure without banding the aorta was also performed in PKD1 cKO (n=7) and WT (n=8) mice.

Isolation of left ventricular cardiomyocytes was performed as previously described.[28] Briefly, animals were injected with heparin (400 U/kg body weight) and anesthetized with isoflurane inhalation (3% to 5%) throughout the procedure. Deep surgical anesthesia was confirmed by abolished pain reflexes. All animals were euthanized by surgical excision of the heart while in deep anesthesia. Immediately after excision, the heart was rinsed in cold nominally Ca^{2+}-free Minimal Essential Medium. The aorta was cannulated and retrograde perfused on constant flow Langendorff apparatus (5 minutes, 37°C) with Ca^{2+}-free normal Tyrode's solution, gassed with 100% O_2. Then, ventricular myocytes were digested using Liberase TM (0.225 mg/mL, Roche). Ventricular myocytes were dispersed and filtered through a nylon mesh then allowed to sediment for 10 minutes. The sedimentation was repeated 3 times using increasing $[Ca^{2+}]$ from 0.125 to 0.25 then 0.5 mmol/L. Finally, ventricular myocytes were kept in Tyrode's solution (0.5 mmol/L $[Ca^{2+}]$) at room temperature until use.

In accordance with the National Institutes of Health initiative,[29] mice of both sexes were used in this study. However, no major sex difference in electrophysiology, hypertrophy, or contractile function was found with a nonsignificant tendency of longer APD, slightly reduced I_{to} and slowly inactivating K+ current ($I_{K,slow}$) in females similar to previous studies in C57BL/6J mice.[30,31] Therefore, the male/female results shown in the article have been merged, and the group comparisons between males and females are shown in Table S1.

Echocardiography

Transthoracic echocardiography was periodically performed in anesthetized (1.5%–3% isoflurane) animals before and after TAC (or sham) surgery. Short axis M-mode images of the left ventricles were acquired using a Vevo 2100 echocardiography system (FUJIFILM VisualSonics, Toronto, ON, Canada) equipped with a 40 MHz transducer. Body temperature was carefully monitored, and anesthesia was adjusted to achieve ≈450 beats/minute heart rate in each animal.

Electrophysiology

Recordings were performed in isolated ventricular cardiomyocytes using whole-cell patch-clamp with physiological solutions at 37°C (for ionic composition, see Data S1). Action potentials (APs) were evoked with short suprathreshold depolarizing pulses at 1 to 10 Hz pacing frequencies in current-clamp experiments.[32] K+ currents were recorded using 10 mmol/L EGTA (free $[Ca^{2+}]_i$=100 nmol/L) in the pipette solution, and in the presence of Na+ and Ca^{2+} channel inhibitors (10 μmol/L tetrodotoxin for voltage-gated Na+ channel, and 10 μmol/L nifedipine for L-type Ca^{2+} channel) in the bath solution. Different K+ current components were separated using biexponential fits (R^2>0.9 in each case) of the time-dependent decay of the voltage-gated K+ current and selective K+ channel inhibitors (Figure S1) as described.[23,28,33] The rapid delayed rectifier K+ current (I_{Kr}) and I_{K1} were sensitive to 1 μmol/L E-4031 and 300 μmol/L Ba^{2+}, respectively. Ionic currents were normalized to cell capacitance, determined in each cell using short (10 milliseconds) hyperpolarizing pulses from –10 to –20 mV.

Transcript Analysis

Total RNA was isolated from PKD1 cKO and WT littermate mouse hearts 8 weeks after TAC or sham surgery (N=3 hearts in each group) using RNeasy Mini Kit (Qiagen). Conversion to cDNA was performed using QuantiTect Reverse Transcription Kit (Qiagen). Transcript analysis of genes encoding K+ channel pore forming and auxiliary subunits, markers of cardiomyocyte hypertrophy (β-myosin heavy chain; atrial natriuretic peptide), as well as housekeeping control genes, including glyceraldehyde 3-phosphate dehydrogenase, S18 ribosomal protein, and hypoxanthine guanine phosphoribosyl transferase was carried out using real-time quantitative polymerase chain reaction on an Applied Biosystems 7900HT Fast Real-Time PCR System and Primer-Probe detection.[28] Three technical replicates were performed for each biological sample. The primers were from Eurofins Genomics and their sequences are provided in Table S2. Transcript data were normalized to the arithmetic mean of glyceraldehyde 3-phosphate dehydrogenase and S18 and analyzed using the threshold cycle (C_T) relative quantification method, then linearized ($2^{-\Delta CT}$) to make comparison.

Statistical Analysis

Data are presented as mean±SEM. Because multiple cells may come from 1 animal, we performed hierarchical statistical analysis taking into account intersubject variability. Statistical significance of differences for continuous variables was tested by a linear-mixed model using nested ANOVA followed by a post hoc Tukey test. Categorical outcomes were evaluated using Fisher's exact test. GraphPad Prism 9 was used for data analysis. Differences were considered statistically significant if $P<0.05$.

RESULTS

PKD1 Upregulation and Cardiac Hypertrophy in TAC-Induced HF

Figure 1A and 1B show a simplified schematic of PKD signaling in cardiomyocytes and the timeline of study protocol. At 8 weeks post-TAC, PKD1 gene (Prkd1) expression was significantly increased in WT
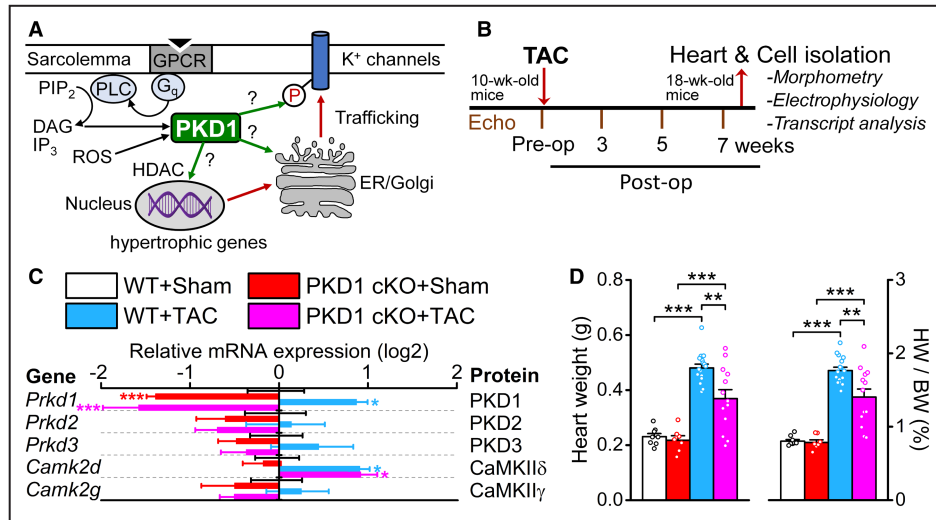
Figure 1. PKD1 signaling and attenuated cardiac hypertrophy after transverse aortic constriction in PKD1 cKO mice.
A, Schematic of PKD1 (protein kinase D1) signaling and potential mechanisms of K+ channel regulation. PKD1 gets activated by G_q-protein coupled receptor (GPCR) stimulation (enhanced in cardiac hypertrophy and heart failure) and regulates several intracellular processes, including gene transcription, intracellular trafficking, and phosphorylates target proteins, all of which may lead to alterations in K+ channel expression and gating. **B**, Timeline of the study protocol. Heart tissues were collected, and cardiomyocytes were isolated from wild-type (WT) and PKD1 cardiomyocyte-specific knockout (cKO) mice 8 weeks after transverse aortic constriction (TAC) or sham procedure. **C**, mRNA expression of PKD1, PKD2, PKD3, CaMKIIδ, and CaMKIIγ relative to WT+Sham. **D**, Heart weight and heart weight/body weight ratio (HW/BW). (WT+Sham: n=8, PKD1 cKO+Sham: n=7, WT+TAC: n=16, and PKD1 cKO+TAC: n=13 animals.) ANOVA with Tukey post hoc test. *$P<0.05$, **$P<0.01$, ***$P<0.001$. CaMKIIδ indicates Ca^{2+}/calmodulin-dependent kinase IIδ; CaMKIIγ Ca^{2+}/calmodulin-dependent kinase IIγ; DAG, diacylglycerol; ER, endoplasmic reticulum; HDAC, histone deacetylase; IP_3, inositol 1,4,5-trisphosphate; PIP_2, phosphatidylinositol 4,5-bisphosphate; PLC, phospholipase C; and ROS, reactive oxygen species.

whole-heart homogenates, whereas no change in PKD2 and PKD3 expression was found (Figure 1C). The expression of Ca^{2+}/calmodulin-dependent protein kinase IIδ (CaMKIIδ) gene (Camk2d) was significantly and similarly increased post-TAC in both WT and PKD1 cKO, but CaMKIIγ gene (Camk2g) expression was unchanged (Figure 1C). At 8-week post-TAC, the heart weight and heart weight/body weight ratio were significantly increased in both WT and PKD1 cKO; however, the extent of cardiac hypertrophy post-TAC was attenuated in PKD1 cKO (Figure 1D).

PKD1 Deletion Attenuates Hypertrophy and Early Decline in Contractile Function in TAC But Does Not Prevent HF Development

Ventricular remodeling and contractile function were periodically assessed by echocardiography after TAC (Figure 2). At 3 weeks post-TAC, representing the early hypertrophic remodeling phase, the ejection fraction was significantly decreased in WT but not in PKD1 cKO. However, at 7 weeks post-TAC when the disease progressed to HF, ejection fraction was similarly decreased in both WT and PKD1 cKO (Figure 2A and 2B). In line with this, significant ventricular dilatation (left ventricular internal diameter at diastole) was found in both WT and PKD1 cKO (Figure 2C, left). In contrast, thickening of the left ventricular posterior wall diameter at diastole post-TAC was found only in WT but not in PKD1 cKO (Figure 2C, right). These results indicate that PKD1 indeed affects ventricular hypertrophy and promotes early remodeling with functional deterioration as previously shown[7]; however, PKD1 cKO does not prevent chronic HF development. In fact, the decline in ejection fraction could be even more rapid in PKD1 cKO between the 3- and 7-week time points post-TAC.

PKD1 Reduces K+ Currents in TAC-Induced HF

Membrane capacitance of the isolated ventricular cardiomyocytes was significantly increased 8 weeks post-TAC in WT (by 77% versus sham) indicating cellular hypertrophy, which was attenuated in PKD1 cKO (51% increase in TAC versus sham). Ionic currents were normalized to the cell capacitance measured in each cell (Figure 3A).
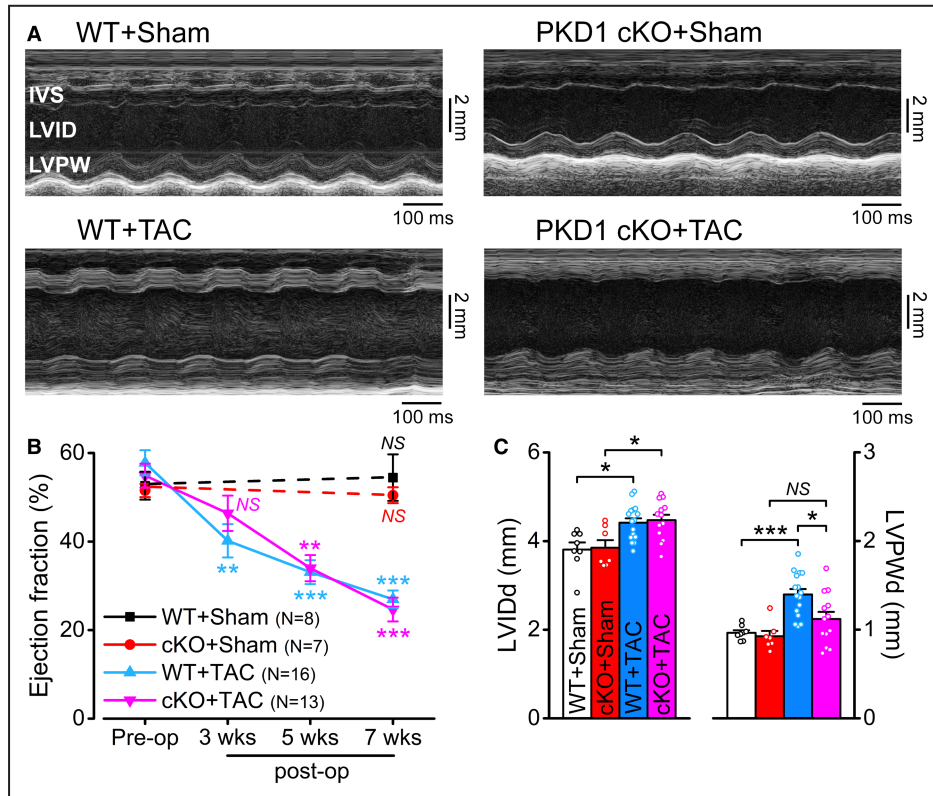
Figure 2. Echocardiographic assessment of WT and PKD1 cKO murine hearts after transverse aortic constriction.
A, Representative echocardiographic M-mode images in WT and PKD1 cKO mice 7 weeks after transverse aortic constriction (TAC) or sham. **B**, Progression of changes in ejection fraction after TAC or sham. Dunnett's test, **$P<0.01$, ***$P<0.001$. **C**, Left ventricular internal dimension at end-diastole (LVIDd) and left ventricular posterior wall thickness at end-diastole (LVPWd) 7 weeks after TAC. (WT+Sham: n=8, PKD1 cKO+Sham: n=7, WT+TAC: n=16, and PKD1 cKO+TAC: n=13 animals.) ANOVA with Tukey post hoc test. *$P<0.05$, ***$P<0.001$. cKO indicates cardiomyocyte-specific knockout; IVS, interventricular septum; PKD1, protein kinase D1; and WT, wild type.

To characterize electrophysiological remodeling, we first measured the major K⁺ currents in isolated murine ventricular cardiomyocytes. The total voltage-gated K⁺ current (I_{Kv}) density was significantly decreased 8 weeks post-TAC in WT (Figure 3B and 3C). I_{Kv} density was larger in PKD1 cKO post-TAC; however, I_{Kv} was also larger in sham PKD1 cKO versus WT. Next, the components of I_{Kv} were separated using 4-AP treatment and biexponential fit to the current decay (Figure S1). I_{to}, $I_{K,slow}$, and I_{sus} were all reduced post-TAC in WT with a marked decrease in I_{to} density (Figure 3D through 3F). Importantly, I_{to} was larger in PKD1 cKO (versus WT) both in sham and TAC (Figure 3D). In contrast, similar downregulation in $I_{K,slow}$ was found post-TAC in both WT and PKD1 cKO (Figure 3E). The noninactivating, sustained K⁺ current (I_{sus}) was slightly reduced post-TAC in WT but remained unchanged in PKD1 cKO (Figure 3F). The time course of I_{to} inactivation was similar in all groups (Figure 3G). However, the recovery from inactivation was significantly slower in WT+TAC

but this change was attenuated in PKD1 cKO+TAC (Figure 3H). I_{K1} density was similar in WT and cKO at baseline but was significantly decreased post-TAC in WT (by 47% at −140 mV), less so in PKD1 cKO (31% reduction at −140 mV; Figure 4A and 4B). I_{Kr} is a tiny current in murine ventricular myocytes (Figure S1C), and I_{Kr} further decreased post-TAC in WT but not in PKD1 cKO (Figure S2A and S2B). I_{Kr} deactivation time constants were similar among groups (Figure S2B).

In WT+TAC myocytes, 10-minute treatment with CRT0066101 (1 μmol/L), a selective PKD inhibitor,[34] slightly increased I_{to} density (by 22%) and sped its recovery from inactivation, but other K⁺ current parameters were unchanged (Figure S3). Interestingly, CRT0066101 also slightly increased I_{to} (by 12%) in WT+Sham myocytes (Figure S4). These data suggest that I_{to} amplitude and recovery from inactivation are regulated—in part—by an acute PKD1-dependent mechanism (eg, via phosphorylation of the corresponding K⁺ channels). Nonetheless, most of the K⁺
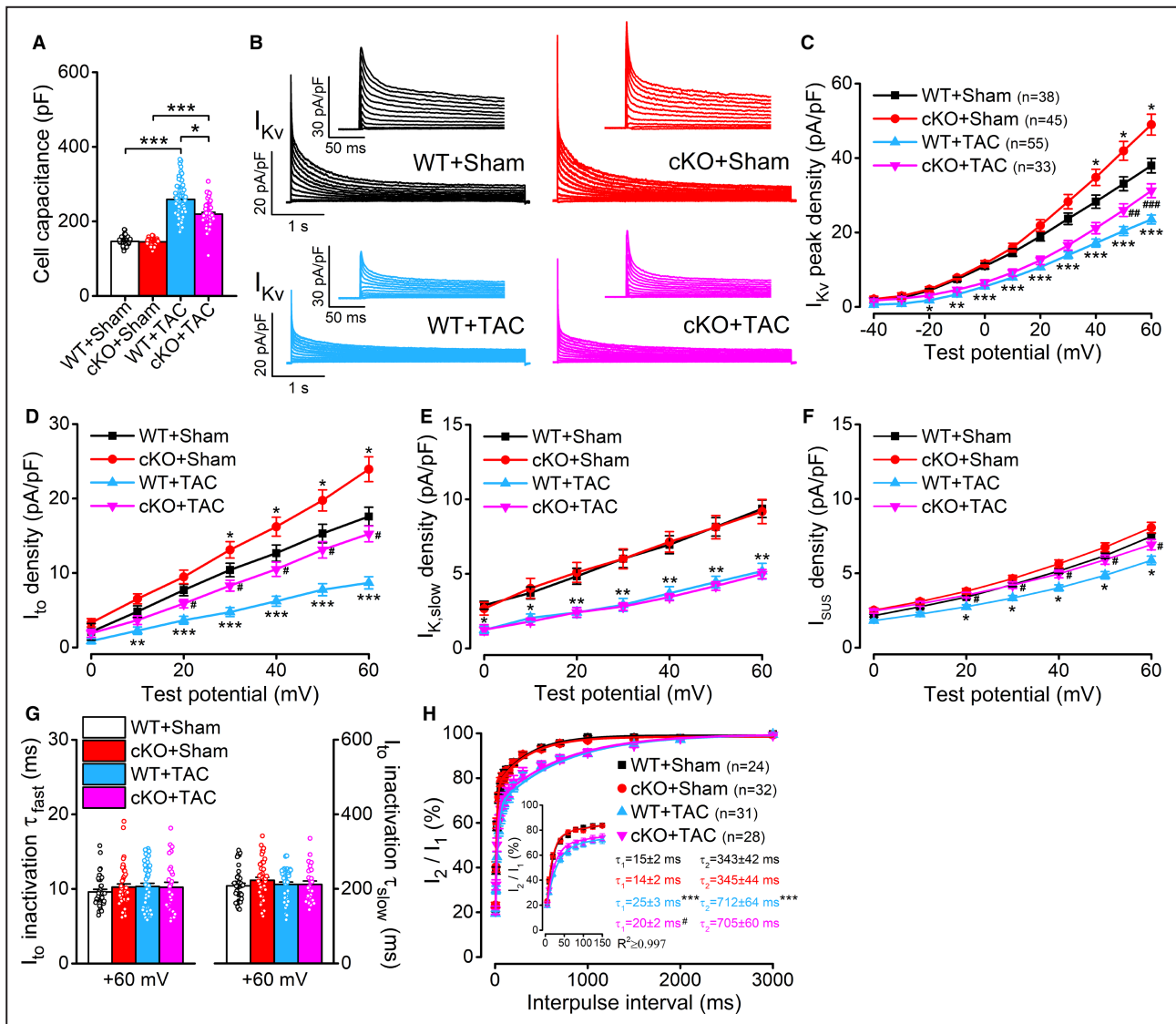
Figure 3. PKD1-dependent remodeling of cardiac voltage-gated K⁺ currents in heart failure.
A, Membrane capacitance of wild-type (WT) and protein kinase D1 cardiomyocyte-specific knockout (PKD1 cKO) ventricular cardiomyocytes 8-week after transverse aortic constriction (TAC) or sham. **B**, Representative voltage-gated outward K⁺ current (I_{Kv}) traces. Early phase of I_{Kv} representing the fast, transient outward K⁺ current (I_{to}) is enlarged in inset. **C**, Peak I_{Kv} density. **D**, I_{to} density. **E**, Slowly inactivating K⁺ current ($I_{K,slow}$) density. **F**, Sustained K⁺ current (I_{sus}) density. **G**, Inactivation time constant of I_{to} (τ_{fast} and τ_{slow}). **H**, I_{to} recovery from inactivation. Fast recovery shown in inset. (Number of animals, WT+Sham: 8, PKD1 cKO+Sham: 5, WT+TAC: 6, and PKD1 cKO+TAC: 5. The number of cells (n) in each experimental group is listed in the figure.) Nested ANOVA with Tukey post hoc test. *$P<0.05$, **$P<0.01$, ***$P<0.001$ vs WT+Sham; #$P<0.05$, ##$P<0.01$, ###$P<0.001$ vs WT+TAC.

current downregulation in TAC-induced HF likely reflects PKD1-dependent regulation of gene transcription (eg, via phosphorylation of histone deacetylases).

PKD1 Contributes to K⁺ Channel Downregulation in TAC-Induced HF

The TAC-induced reduction in K⁺ current densities may result from a decrease in total sarcolemmal K⁺ channel expression or a mismatch between increased cell volume (hypertrophy) and K⁺ channel synthesis.[23] Therefore, we examined the relationship between the net amplitude per myocyte, the density (amplitude normalized to cell capacitance), and mRNA level of each K⁺ channel. For net K⁺ current amplitudes per myocyte, none of the K⁺ current amplitudes were reduced in WT+TAC, and I_{sus} was even increased in WT+TAC versus WT+Sham (Figure 5A). However, $I_{K,slow}$ amplitude was reduced only in PKD1 cKO+TAC. The net I_K amplitude was the same post-TAC in both WT and PKD1 cKO, whereas it was increased in PKD1 cKO+Sham because of the larger I_{to} amplitude (Figure 5A). Thus, TAC alone failed to alter the amount of K⁺ current per myocyte appreciably, but the observed myocyte
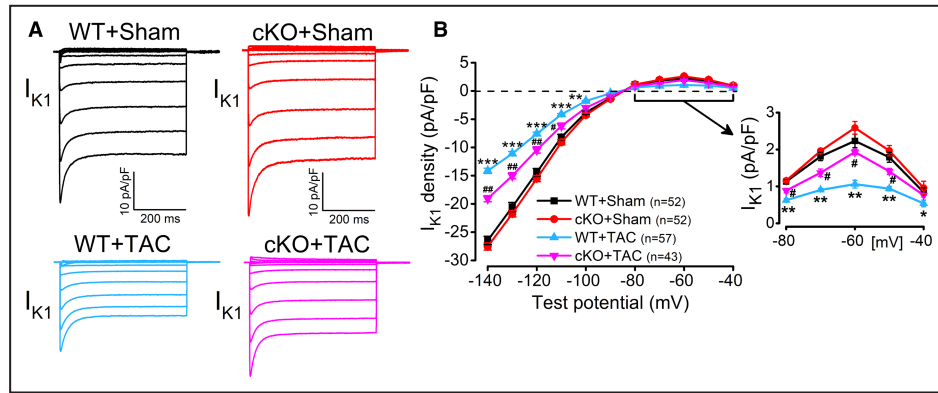
Figure 4. PKD1-dependent remodeling of cardiac inward rectifier K⁺ current in heart failure.
A, Representative inward rectifier K⁺ current (I_{K1}) traces. **B**, I_{K1} density-voltage relationship. Outward component is enlarged in inset. (Number of animals, WT+Sham: 8, PKD1 cKO+Sham: 5, WT+TAC: 6, and PKD1 cKO+TAC: 5. The number of cells (n) in each experimental group is listed in the figure.) Nested ANOVA with Tukey post hoc test. *$P<0.05$, **$P<0.01$, ***$P<0.001$ vs WT+Sham; #$P<0.05$, ##$P<0.01$, ###$P<0.001$ vs WT+TAC. cKO indicates cardiomyocyte-specific knockout; PKD1, protein kinase D1; TAC, transverse aortic constriction; and WT, wild type.

hypertrophy (Figure 3A) would tend to dilute the current density. Indeed, when K⁺ current was normalized to cell capacitance (a measure of membrane surface area) as is typical for electrophysiology, the density of all 5 K⁺ currents (in pA/pF) was reduced in TAC (Figure 5B).

Expression analysis of the major murine myocardial K⁺ channel mRNAs 8 weeks post-TAC revealed downregulation of Kcnd2, Kcnip2, Kcna5, Kcnk3, Kcnj2, and Kcnh2a/b (Figure 5C) and upregulation of myocyte hypertrophy markers (β-myosin heavy chain and atrial natriuretic peptide) in WT+TAC (Figure S5). Importantly, PKD1 cKO+TAC showed no change in Kcnj2 and Kcnh2a/b (mediating I_{K1} and I_{Kr}), less downregulation in Kcnd2, Kcnip2 (mediating I_{to}) and Kcnk3 (mediating I_{sus}), and less upregulation of β-myosin heavy chain versus WT+TAC (Figure 5C; Figure S5). Kcna5 (mediating $I_{K,slow}$) was significantly downregulated post-TAC in both WT and PKD1 cKO (Figure 5C). All these changes in the expression of K⁺ channels post-TAC mirror the changes in K⁺ current densities.

PKD1 Contributes to Impaired AP Repolarization in TAC-Induced HF

Figure 6 shows representative APs in WT and PKD1 cKO cardiomyocytes 8 weeks post-TAC under physiological condition where myocyte $[Ca^{2+}]_i$ transients and contraction were allowed (Figure 6A) and when $[Ca^{2+}]_i$ was buffered to 100 nmol/L using 10 mmol/L EGTA in the pipette (Figure 6B). TAC (at 8 weeks) prolonged AP duration at 90% repolarization (APD_{90}) in WT at all pacing frequencies (1–10 Hz) under both physiological conditions and with $[Ca^{2+}]_i$ held at 100 nmol/L (Figure 6C and 6D). In PKD1 cKO the APD_{90} prolongation post-TAC was

attenuated at slow pacing frequencies (1–5 Hz, Figure 6C) in line with faster early repolarization (Figure 6A) and higher I_{to} density (Figure 3D). Of note, APD_{90} in sham was slightly shorter in PKD1 cKO, independent of $[Ca^{2+}]_i$ transient (Figure 6C and 6D). The resting membrane potential was depolarized by TAC in WT, but this was attenuated in PKD1 cKO+TAC (Figure 6E), which would be in line with the changes in the density of I_{K1} (which is key in stabilizing the myocyte resting membrane potential). The AP amplitude was reduced in WT+TAC but not in PKD1 cKO+TAC (Figure 6F), which might be due to I_{K1} and resting membrane potential changes and could influence Na⁺ channel availability.

Both WT and PKD1 cKO exhibited APD alternans post-TAC at rapid pacing frequencies (9–10 Hz) when $[Ca^{2+}]_i$ transient was preserved (see bifurcations in Figures 6C and 7), indicating an important Ca^{2+}-dependent arrhythmogenic mechanism. Moreover, beat-to-beat and short-term variabilities of APD_{90} were significantly increased in WT+TAC even at 1 Hz steady-state pacing (Figure 7E), and the number of subsequent beats having >5 and >10 milliseconds difference in APD_{90} was markedly increased (Figure 7F). Importantly, this increased beat-to-beat variability at lower pacing frequencies was prevented in PKD1 cKO+TAC (Figure 7F), but the tachypacing-induced alternans was not (Figure 7C).

PKD1 Enhances Spontaneous Arrhythmogenic Activities in TAC-Induced HF

Arrhythmogenic diastolic activities were elicited by cessation of 1-minute tachypacing at 10 Hz (Figure 8A). The fraction of cells exhibiting delayed afterdepolarization (DAD), spontaneous AP, and early afterdepolarization
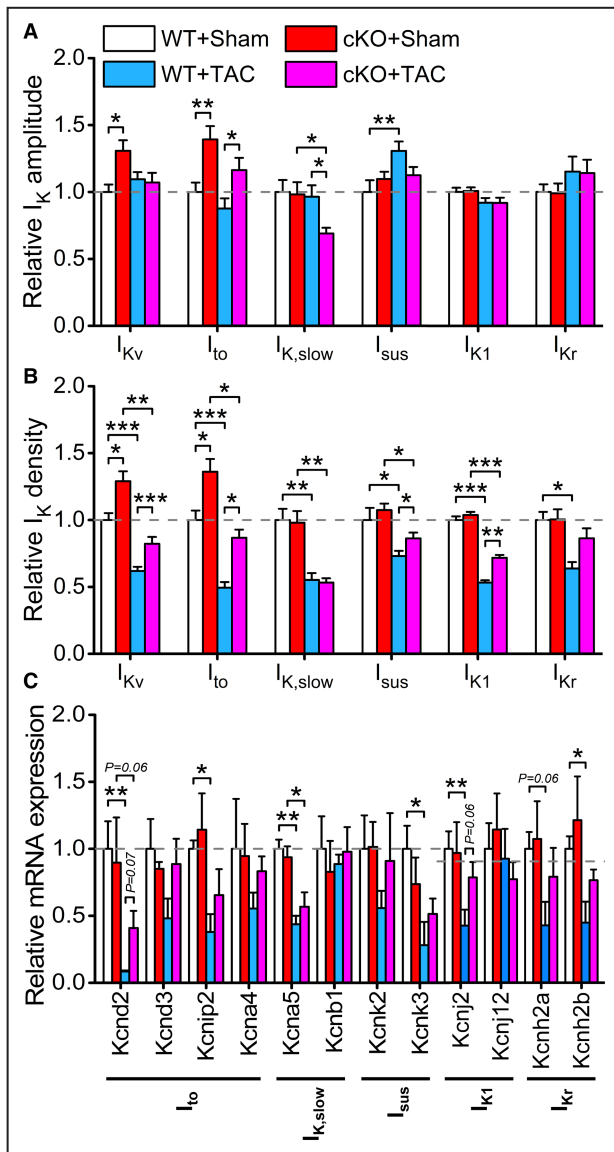
Figure 5. Relative changes in K+ currents and expression of corresponding K+ channel genes.
A, Net K+ current amplitudes normalized to WT+Sham. **B**, K+ current densities normalized to WT+Sham. **C**, Expression of K+ channel subunits normalized to WT+Sham (n=3 hearts in each experimental group, and 3 technical replicates have been performed for each heart). Nested ANOVA with Tukey post hoc test. *$P<0.05$, **$P<0.01$, ***$P<0.001$. cKO indicates cardiomyocyte-specific knockout; I_{K1}, inward rectifier K+ current; $I_{K,slow}$, slowly inactivating K+ current; I_{Kr}, rapid delayed rectifier K+ current; I_{Kv}, total voltage-gated outward K+ current; I_{sus}, sustained K+ current; I_{to}, fast, transient outward K+ current; PKD1, protein kinase D1; TAC, transverse aortic constriction; and WT, wild type.

superimposed on the spontaneous AP repolarization phase (complex spontaneous AP) was significantly increased in WT+TAC versus WT+Sham (Figure 8B). The frequency of these arrhythmogenic events was also significantly increased in WT+TAC (Figure 8C). However, these spontaneous diastolic events were less frequent

in PKD1 cKO+TAC (Figure 8C). None of these arrhythmogenic events were observed in cells measured with 10 mmol/L EGTA in the pipette (Figure S6A), indicating a critical role for spontaneous Ca^{2+} release from the sarcoplasmic reticulum (SR). DAD amplitude was increased post-TAC in both WT and PKD1 cKO, but the increase was more pronounced in WT (Figure 8D; Figure S6B and S6C) consistent with the changes in I_{K1} density (Figure 4B). The increase in DAD amplitude also correlated positively with cellular hypertrophy (Figure S6D).

DISCUSSION

PKD1 Mediates Hypertrophic Signaling and Cardiac Remodeling

Cardiac hypertrophy and remodeling usually develop upon sustained cardiac stress. The underlying signaling pathways including PKD1 and CaMKIIδ among others have been extensively studied, and their inhibition has been suggested as a potential therapeutic targets to prevent cardiac hypertrophy and its maladaptive consequences leading to HF and arrhythmias.[5–8,10,11,14,27,35,36] Notwithstanding the accumulated evidence of cellular signaling studies, further in vivo target validation of PKD1 is needed. Importantly, PKD1 cKO mice were found to be resistant to early cardiac hypertrophy, fibrosis, and functional deterioration induced by either pressure overload or chronic infusion with isoproterenol or angiotensin II.[7] The naphthyridine and bipyridine pan-PKD inhibitors could not reduce cardiac hypertrophy in Dahl salt sensitive rats or mice with abdominal aortic banding,[37,38] although this could result from opposing roles of PKD isoforms (as seen in cancer[39]) or off-target drug effects. In the present study, we showed that upon chronic TAC-induced pressure overload, PKD1 cKO mice also exhibited significantly reduced hypertrophy (Figure 1) and prevented the early decline in cardiac contractile function (Figure 2) in line with previous report.[7] However, chronic pressure overload still led to HF in PKD1 cKO mice (Figure 2), suggesting that prevention of hypertrophy is ultimately not sufficient to prevent HF development and progression. This is in accordance with a previous study using a truncated version of AKAP13 (A-kinase anchoring protein 13)-Lbc, which abolished its interaction with PKD1, resulting in reduced PKD1 activation by short-term pressure overload or infusion with either angiotensin II or phenylephrine; which led to reduced compensatory cardiac hypertrophy but enhanced progression of HF.[26] These data may indicate a possible mechanism for "compensatory" hypertrophy, mediated by PKD1 signaling, though the existence of "compensatory" hypertrophy is still debated clinically.[13,17] APD
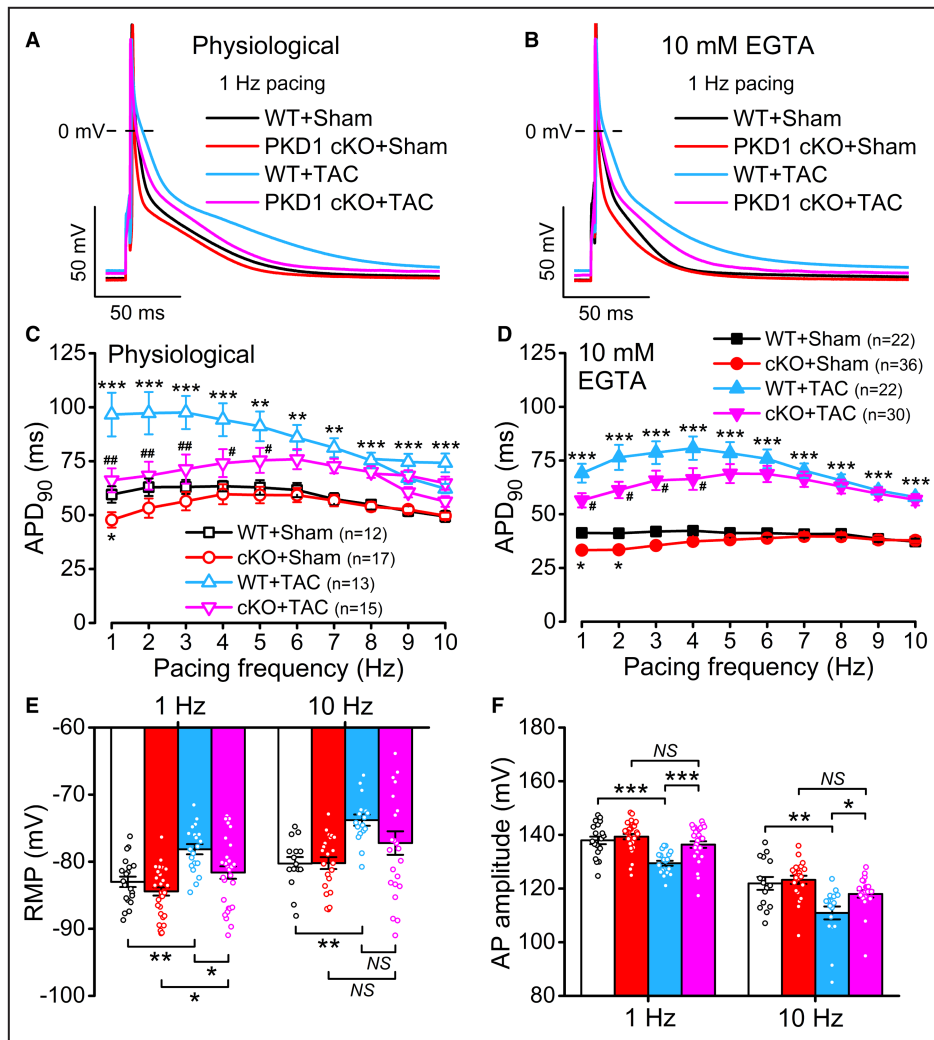
Figure 6. PKD1 enhances proarrhythmic action potential remodeling in heart failure.
A, Representative action potentials (APs) measured under physiological conditions (without using exogenous Ca^{2+} buffers, at 37°C) in isolated left ventricular cardiomyocytes 8 weeks post-TAC. **B**, Representative APs measured when cytosolic Ca^{2+} concentration was buffered to 100 nmol/L with 10 mmol/L EGTA. **C**, Frequency-dependence of AP duration at 90% of repolarization (APD_{90}) under physiological conditions. **D**, Frequency-dependence of APD_{90} with buffered cytosolic Ca^{2+}. **E**, Resting membrane potential (RMP) at 1 and 10 Hz pacing. **F**, AP amplitude was reduced in HF. (Number of animals, WT+Sham: 8, PKD1 cKO+Sham: 5, WT+TAC: 6, and PKD1 cKO+TAC: 5. The number of cells (n) in each experimental group is listed in the figure.) Nested ANOVA with Tukey post hoc test. *$P<0.05$, **$P<0.01$, ***$P<0.001$ vs WT+Sham; #$P<0.05$, ##$P<0.01$ vs WT+TAC. cKO indicates cardiomyocyte-specific knockout; HF, heart failure; PKD1 protein kinase D1; TAC, transverse aortic constriction; and WT, wild type.

prolongation and shape (as a consequence of K⁺ channel downregulation) may also have some compensatory effects by increasing the Ca^{2+} transient and providing positive inotropy; however, this may also promote the late Ca^{2+} handling impairments during HF progression.[40] In line with this, transgenic mice expressing cardiomyocyte-specific dominant-negative $K_V4.2$ channels showed reduced I_{to} magnitude and a healthy cardiac phenotype at birth but developed significant congestive HF by 12 to 13 weeks of age.[41]

Interestingly, the roles we have identified for PKD1 (a member of the CaM kinase superfamily based on similarities in the catalytic domain) in mediating cardiac hypertrophy and HF contrasts with the previously identified roles of CaMKIIδ in HF. CaMKIIδ KO mice were resistant to HF development and its arrhythmogenic consequences but did not reduce early cardiac hypertrophy induced by TAC.[27,35,36] Moreover, early CaMKIIδ activation was prominent in the perinuclear region very early in TAC and caused a compensatory increase in
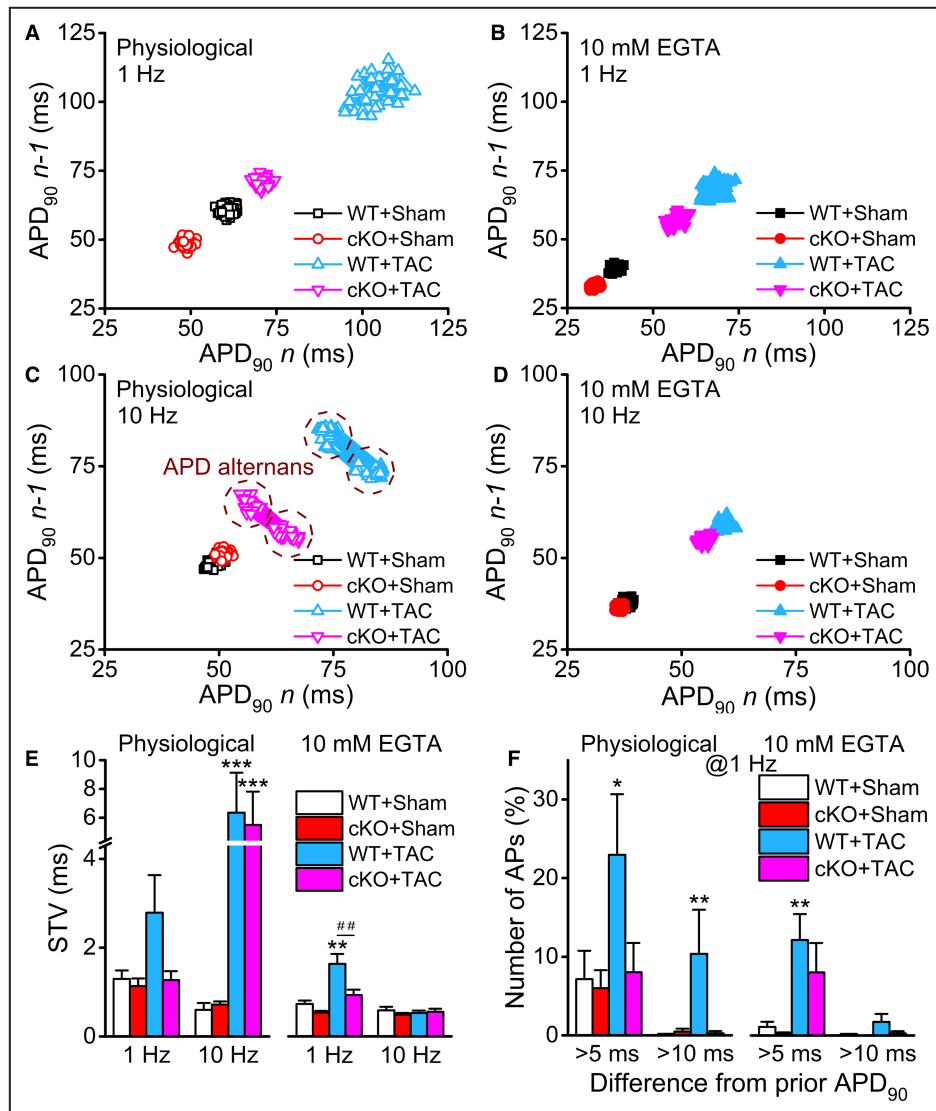
Figure 7. Temporal variability of action potential duration in WT and PKD1 cKO failing myocytes.

A and **B**, Representative Poincare plots of 50 consecutive action potential duration at 90% repolarization (APD_{90}) values obtained in isolated ventricular cardiomyocytes at 1 Hz pacing frequency under physiological conditions (with preserved $[Ca^{2+}]_i$ transient) and when $[Ca^{2+}]_i$ was buffered to 100 nmol/L using 10 mmol/L EGTA in the pipette. **C** and **D**, Representative Poincare plots obtained at 10 Hz pacing frequency. Under physiological conditions, significant APD_{90} alternans (short-long-short-long APDs) occurred post-TAC in both WT and PKD1 cKO. **E**, Frequency-dependent short-term variability (STV) of APD_{90}. Nested ANOVA with Tukey post hoc test. **$P<0.01$, ***$P<0.001$ vs WT+Sham; ##$P<0.01$ vs WT+TAC. n/N=12–36 cells/3–7 animals. **F**, Percentage of all APs measured at 1 Hz pacing having beat-to-beat APD_{90} variability of >5 milliseconds and >10 milliseconds in consecutive beats. Action potentials were recorded under physiological conditions (*left*) and using 10 mmol/L EGTA (free $[Ca^{2+}]_i$=100 nmol/L) in the pipette solution (*right*). Fisher's exact test. **$P<0.01$. AP indicates action potential; cKO cardiomyocyte-specific knockout; PKD1 protein kinase D1; TAC, transverse aortic constriction; and WT, wild type.

SR Ca^{2+} content and $[Ca^{2+}]_i$ transient amplitude; however, the enhanced histone deacetylase 4 nuclear export and nuclear transcriptional responses still contributed to eccentric hypertrophy and HF.[14] An intriguing question is to identify the mechanism responsible

for the different functional outcomes in PKD1 KO versus CaMKIIδ KO in their adaptations to chronic cardiac stress. Regulation of transcription by PKD1 and CaMKIIδ has been reported to share similar features (eg, phosphorylation and nuclear export of class II
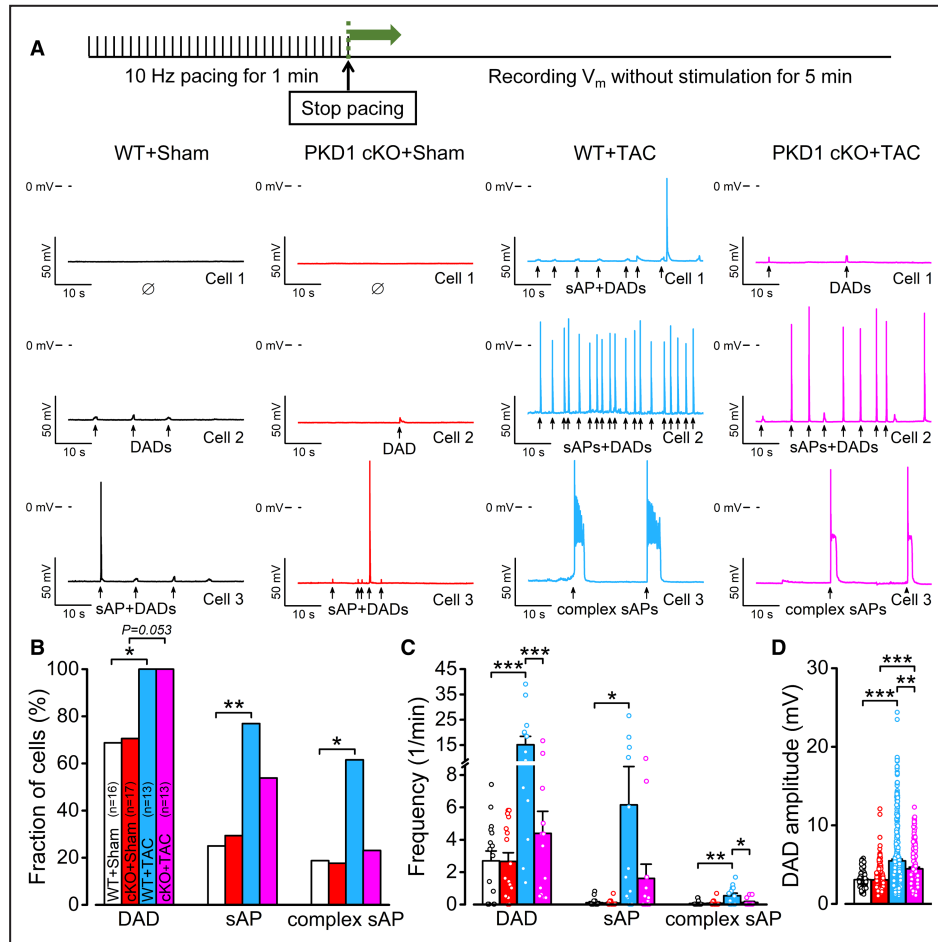
Figure 8. Arrhythmogenic diastolic activities in WT and PKD1 cKO failing myocytes.
A, Arrhythmogenic diastolic activities were elicited using a tachypacing protocol. Representative records of 3 cells in each experimental group are shown. **B**, Percentage of cells exhibiting delayed afterdepolarizations (DADs), spontaneous action potential (sAP) and complex sAP (early afterdepolarization superimposed on sAP). Fisher's exact test. *$P<0.05$, **$P<0.01$. **C**, Frequency of the arrhythmogenic diastolic activities. **D**, Amplitude of DADs. (Number of animals, WT+Sham: 8, PKD1 cKO+Sham: 5, WT+TAC: 5, and PKD1 cKO+TAC: 5. The number of cells (n) in each experimental group is listed in the figure.) Nested ANOVA with Tukey post hoc test. **$P<0.01$, ***$P<0.001$. cKO indicates cardiomyocyte-specific knockout; PKD1 protein kinase D1; TAC, transverse aortic constriction; and WT, wild type.

histone deacetylases)[5,42]; however, subtle differences in phosphorylated histone deacetylase isoforms[43] and other targets (eg, histone H3 phosphorylation by CaMKIIδ[44]) also exist. Modulation of $Ca_v1.2$ channels and contractile proteins (eg, troponin I, myosin binding protein-C) have also been shown for both PKD1 and CaMKIIδ, see recent reviews.[3,45] Some aspects of our observations of PKD1-dependent K+ channel downregulation (Figure 5) also resemble the chronic CaMKIIδ-dependent effects (eg, downregulations of I_{to} and I_{K1}).[28,46] However, unlike CaMKIIδ,[46] PKD1 did not affect $I_{K,slow}$ density (Figure 3), but reduced I_{sus} and I_{Kr} (Figure 3; Figure S2). Another important mechanism in cardiac dysfunction is the increased SR Ca^{2+} leak in HF,[47] which leads to enhanced DAD susceptibility

post-TAC (Figure 8). Importantly, CaMKIIδ but not PKD1 has been previously shown to phosphorylate ryanodine receptors, which promotes spontaneous diastolic SR Ca^{2+} release and triggers arrhythmias.[48–50] These differences for PKD1 and CaMKIIδ highlight the need to further unravel their respective molecular roles in cardiac hypertrophy and HF, in order to empower the pursuit of rationally designed treatments for cardiac hypertrophy and arrhythmias.

PKD1 Mediates K+ Channel Remodeling in Cardiac Hypertrophy and HF

K+ channel remodeling is an important arrhythmogenic sequela of cardiac hypertrophy and HF.[20–22] The extent

of downregulation in some K^+ currents closely followed the changes in cell dimensions (eg, I_{to} and I_{K1}), whereas I_{sus} downregulation was less prominent in HF (Figure 5), in accordance with a previous report on TAC-induced early cardiac hypertrophy.[23]

PKD-dependent regulation of K^+ channels has already been implicated in 2 previous studies[25,51]; however, the exact contribution of PKD in modulating cardiac K^+ currents remained elusive. In diet-induced obesity, upregulated PKD was associated with reduced CREB expression and downregulation of $K_V1.5$ and $K_V2.1$ channel expression in the heart.[25] However, others reported that PKD activation led to CREB S133 phosphorylation, activation of a CRE-responsive promoter, and increased Bcl-2 (CREB target gene) expression in cardiomyocyte cultures.[52] Here, we found a decreased I_{to} and $I_{K,slow}$ post-TAC (Figure 3) and downregulation of multiple K^+ channel subunits (poreforming Kcnd2, Kcna5, and important auxiliary subunit KChIP2; Figure 5C); This is in line with numerous previous reports examining the effects of TAC on K^+ channels (see reviews[20,22] for details). Interestingly, PKD1 affected the expression of Kcnd2/$K_V4.2$ but not Kcna5/$K_V1.5$, as was suggested previously.[25] The exact molecular mechanisms by which PKD1 regulates the transcription of K^+ channels, including identification of transcription factors involved and their specific transcriptome profiles, require further investigation.

Acute and selective inhibition of PKD with CRT0066101 slightly increased I_{to} and enhanced the slow recovery from inactivation (Figure S3), suggesting a direct PKD action on gating of these K^+ channels, in addition to gene expression changes (side note: although the cardiac antihypertrophic effect of CRT0066101 has not yet been assessed, we did not use the naphthyridine or bipyridine PKD inhibitors here as they are not readily available). Serine-557 on $K_v1.5$, S524 on $K_V4.2$ and S437 on $K_V4.3$ sites all conform to the PKD phosphorylation consensus sequence (L/V/I-X-R/K-X-X-S/T). Of note, S557 on $K_V1.5$ was thought to be a protein kinase A site,[53] whereas to date phosphorylation of the other 2 residues has not been reported. Alternatively, PKD is also known to regulate the trans-Golgi network and may affect K^+ channel trafficking.[54] Indeed, PKD1 has been shown to regulate $K_V11.1$ (Kcnh2/human ether-a-go-go-related gene/I_{Kr}) channels, which may involve the phosphorylation of S284 leading to reduced current amplitude, but interestingly without altering surface protein expression or the biophysical properties of the human ether-a-go-related gene channel expressed in human embryonic kidney-293 cells.[51] Furthermore, the human ether-a-go-go-related gene promoter has been shown to be regulated by CREB.[25] Accordingly, we found PKD1-dependent downregulation of I_{Kr} and corresponding reduction in Kcnh2a and Kcnh2b expression post-TAC

(Figure S2; Figure 5C). Importantly, here we demonstrated that downregulations of I_{K1}/Kcnj2/$K_{ir}2.1$ and I_{sus}/Kcnk3/Task-1 were also partially PKD1 dependent (Figures 3–5). Although murine ventricular AP morphology and K^+ channel expression pattern significantly differ from that of humans, downregulation of I_{to}, I_{K1}, and I_{Kr} have all been demonstrated in human HF[20] and are important determinants of human AP repolarization[55] providing translational value to our study. Moreover, recently a powerful computational framework has been established for interspecies translation of electrophysiology and Ca^{2+} handling from mouse to human.[56]

PKD1 Signaling and Arrhythmias in Cardiac Hypertrophy and HF

Cardiac hypertrophy and HF are associated with remodeling of multiple ion channels in the heart.[20,57] K^+ channel downregulation is among the predominant electrophysiological alterations in HF, which reduces the repolarization reserve and contributes to APD prolongation with increased risk of arrhythmias.[21–24,58] This arrhythmogenic substrate in HF is further enhanced by the increased beat-to-beat variability of APD in which the reduced K^+ currents are involved.[24,59] APD prolongation by itself can also enhance SR Ca^{2+} instability.[60] Importantly, TAC-induced K^+ channel downregulation (Figure 5), APD prolongation (Figure 6) and increased beat-to-beat APD-variability (Figure 7) were all significantly attenuated in PKD1 cKO. Transmural dispersion of repolarization is also known to be altered in cardiac hypertrophy and HF, predominantly because of I_{to} downregulation.[20–23] These results suggest that PKD inhibition might be beneficial in the attenuation of arrhythmogenicity. However, further studies with small molecule PKD inhibitors in HF models are needed to evaluate their therapeutic potential.

Numerous other factors can contribute to arrhythmogenesis. Altered myocyte Ca^{2+} handling and enhanced (CaMKII-dependent) SR Ca^{2+} leak are characteristic of HF,[61] which can increase APD alternans and afterdepolarizations.[47–50] Importantly, DADs were reduced post-TAC in PKD1 cKO (Figure 8) in line with reduced cellular hypertrophy and larger I_{K1} density (Figures 4 and Figure S6). DADs are also promoted by the larger spontaneous Ca^{2+} releases and generally increased Na/Ca exchanger density in HF.[47] Increased APD alternans is an important proarrhythmic mechanism in HF, and APD prolongation and shortened diastolic interval promote alternans formation.[62] Interestingly, APD alternans was not affected by PKD1 cKO (Figure 7) despite the shorter APD in PKD1 cKO after TAC (Figure 6), further suggesting that potentially similar Ca^{2+} handling impairment drives the APD alternans in both WT and PKD1 cKO in HF. PKD is also known to influence fibrosis, mitochondrial function and

cell metabolism,[3,7,63] which in turn may contribute to arrhythmogenesis, but these roles of PKD in HF require further investigation. Clinically, the effects of PKD inhibition must be considered when patients with HF are treated with angiotensin-converting enzyme inhibitors, angiotensin II receptor blockers, and mineralocorticoid receptor antagonists because the affected neurohumoral mediators are increased in HF, significantly upregulate PKD1, and contribute to cardiovascular remodeling. It is clear that the role of PKD1 in cardiac hypertrophy and arrhythmogenesis merits further investigation. Moreover, treatment with the novel, orally bioavailable, selective PKD inhibitors may represent a potential therapeutic option in heart disease.

CONCLUSIONS

Our data show that PKD1 cKO mice exhibit significantly attenuated cardiac hypertrophy and are protected against the early decline in contractile function upon chronic pressure overload via TAC. However, PKD1 cKO did not prevent the development of congestive HF. Nonetheless, PKD1 cKO significantly attenuated K⁺ channel downregulation and proarrhythmic APD changes in HF. These data reveal the nuanced and time-specific role for PKD1 in mediating HF-related hypertrophic response and arrhythmias. Moreover, our data indicate an important mismatch between cardiac hypertrophy-K⁺ channel downregulation-APD prolongation and HF development and progression.

ARTICLE INFORMATION

Affiliation

Department of Pharmacology, University of California, Davis, CA.

Supplemental Material

Data S1
Tables S1–S2
Figures S1–S6

REFERENCES

1. Bossuyt J, Chang CW, Helmstadter K, Kunkel MT, Newton AC, Campbell KS, Martin JL, Bossuyt S, Robia SL, Bers DM. Spatiotemporally distinct protein kinase D activation in adult cardiomyocytes in response to phenylephrine and endothelin. *J Biol Chem*. 2011;286:33390–33400. doi: 10.1074/jbc.M111.246447

2. Avkiran M, Rowland AJ, Cuello F, Haworth RS. Protein kinase D in the cardiovascular system: emerging roles in health and disease. *Circ Res*. 2008;102:157–163. doi: 10.1161/CIRCRESAHA.107.168211

3. Wood BM, Bossuyt J. Emergency spatiotemporal shift: the response of protein kinase d to stress signals in the cardiovascular system. *Front Pharmacol*. 2017;8:9. doi: 10.3389/fphar.2017.00009

4. Steinberg SF. Decoding the cardiac actions of protein kinase D isoforms. *Mol Pharmacol*. 2021;100:558–567. doi: 10.1124/molpharm.121.000341

5. Bossuyt J, Helmstadter K, Wu X, Clements-Jewery H, Haworth RS, Avkiran M, Martin JL, Pogwizd SM, Bers DM. Ca²⁺/calmodulin-dependent protein kinase IIdelta and protein kinase D overexpression reinforce the histone deacetylase 5 redistribution in heart failure. *Circ Res*. 2008;102:695–702. doi: 10.1161/CIRCRESAHA.107.169755

6. Carnegie GK, Soughayer J, Smith FD, Pedroja BS, Zhang F, Diviani D, Bristow MR, Kunkel MT, Newton AC, Langeberg LK, et al. AKAP-Lbc mobilizes a cardiac hypertrophy signaling pathway. *Mol Cell*. 2008;32:169–179. doi: 10.1016/j.molcel.2008.08.030

7. Fielitz J, Kim MS, Shelton JM, Qi X, Hill JA, Richardson JA, Bassel-Duby R, Olson EN. Requirement of protein kinase D1 for pathological cardiac remodeling. *Proc Natl Acad Sci USA*. 2008;105:3059–3063. doi: 10.1073/pnas.0712265105

8. Zhang L, Malik S, Pang J, Wang H, Park KM, Yule DI, Blaxall BC, Smrcka AV. Phospholipase Cepsilon hydrolyzes perinuclear phosphatidylinositol 4-phosphate to regulate cardiac hypertrophy. *Cell*. 2013;153:216–227. doi: 10.1016/j.cell.2013.02.047

9. Herwig M, Kolijn D, Lodi M, Holper S, Kovacs A, Papp Z, Jaquet K, Haldenwang P, Dos Remedios C, Reusch PH, et al. Modulation of titin-based stiffness in hypertrophic cardiomyopathy via protein kinase D. *Front Physiol*. 2020;11:240. doi: 10.3389/fphys.2020.00240

10. Harrison BC, Kim MS, van Rooij E, Plato CF, Papst PJ, Vega RB, McAnally JA, Richardson JA, Bassel-Duby R, Olson EN, et al. Regulation of cardiac stress signaling by protein kinase D1. *Mol Cell Biol*. 2006;26:3875–3888. doi: 10.1128/MCB.26.10.3875-3888.2006

11. McKinsey TA. Derepression of pathological cardiac genes by members of the CaM kinase superfamily. *Cardiovasc Res*. 2007;73:667–677. doi: 10.1016/j.cardiores.2006.11.036

12. Hill JA, Karimi M, Kutschke W, Davisson RL, Zimmerman K, Wang Z, Kerber RE, Weiss RM. Cardiac hypertrophy is not a required compensatory response to short-term pressure overload. *Circulation*. 2000;101:2863–2869. doi: 10.1161/01.cir.101.24.2863

13. Schiattarella GG, Hill TM, Hill JA. Is load-induced ventricular hypertrophy ever compensatory? *Circulation*. 2017;136:1273–1275. doi: 10.1161/CIRCULATIONAHA.117.030730

14. Ljubojevic-Holzer S, Herren AW, Djalinac N, Voglhuber J, Morotti S, Holzer M, Wood BM, Abdellatif M, Matzer I, Sacherer M, et al. CaMKIIdeltaC drives early adaptive Ca²⁺ change and late eccentric cardiac hypertrophy. *Circ Res*. 2020;127:1159–1178. doi: 10.1161/CIRCRESAHA.120.316947

15. Sussman MA, Lim HW, Gude N, Taigen T, Olson EN, Robbins J, Colbert MC, Gualberto A, Wieczorek DF, Molkentin JD. Prevention of cardiac hypertrophy in mice by calcineurin inhibition. *Science*. 1998;281:1690–1693. doi: 10.1126/science.281.5383.1690

16. Olson EN, Molkentin JD. Prevention of cardiac hypertrophy by calcineurin inhibition: hope or hype? *Circ Res*. 1999;84:623–632. doi: 10.1161/01.res.84.6.623

17. Frey N, Katus HA, Olson EN, Hill JA. Hypertrophy of the heart: a new therapeutic target? *Circulation*. 2004;109:1580–1589. doi: 10.1161/01.CIR.0000120390.68287.BB

18. Schiattarella GG, Hill JA. Inhibition of hypertrophy is a good therapeutic strategy in ventricular pressure overload. *Circulation*. 2015;131:1435–1447. doi: 10.1161/CIRCULATIONAHA.115.013894

19. Levy D, Anderson KM, Savage DD, Balkus SA, Kannel WB, Castelli WP. Risk of ventricular arrhythmias in left ventricular hypertrophy: the Framingham Heart Study. *Am J Cardiol*. 1987;60:560–565. doi: 10.1016/0002-9149(87)90305-5

20. Tomaselli GF, Marban E. Electrophysiological remodeling in hypertrophy and heart failure. *Cardiovasc Res*. 1999;42:270–283. doi: 10.1016/s0008-6363(99)00017-6

21. Beuckelmann DJ, Nabauer M, Erdmann E. Alterations of K⁺ currents in isolated human ventricular myocytes from patients with terminal heart failure. *Circ Res*. 1993;73:379–385. doi: 10.1161/01.res.73.2.379

22. Nabauer M, Kaab S. Potassium channel down-regulation in heart failure. *Cardiovasc Res*. 1998;37:324–334. doi: 10.1016/s0008-6363(97)00274-5

23. Marionneau C, Brunet S, Flagg TP, Pilgram TK, Demolombe S, Nerbonne JM. Distinct cellular and molecular mechanisms underlie functional

remodeling of repolarizing K$^+$ currents with left ventricular hypertrophy. *Circ Res*. 2008;102:1406–1415. doi: 10.1161/CIRCRESAHA.107.170050

24. Hegyi B, Bossuyt J, Ginsburg KS, Mendoza LM, Talken L, Ferrier WT, Pogwizd SM, Izu LT, Chen-Izu Y, Bers DM. Altered repolarization reserve in failing rabbit ventricular myocytes: calcium and beta-adrenergic effects on delayed- and inward-rectifier potassium currents. *Circ Arrhythm Electrophysiol*. 2018;11:e005852. doi: 10.1161/CIRCEP.117.005852

25. Huang H, Amin V, Gurin M, Wan E, Thorp E, Homma S, Morrow JP. Diet-induced obesity causes long QT and reduces transcription of voltage-gated potassium channels. *J Mol Cell Cardiol*. 2013;59:151–158. doi: 10.1016/j.yjmcc.2013.03.007

26. Taglieri DM, Johnson KR, Burmeister BT, Monasky MM, Spindler MJ, DeSantiago J, Banach K, Conklin BR, Carnegie GK. The C-terminus of the long AKAP13 isoform (AKAP-Lbc) is critical for development of compensatory cardiac hypertrophy. *J Mol Cell Cardiol*. 2014;66:27–40. doi: 10.1016/j.yjmcc.2013.10.010

27. Ling H, Zhang T, Pereira L, Means CK, Cheng H, Gu Y, Dalton ND, Peterson KL, Chen J, Bers D, et al. Requirement for Ca^{2+}/calmodulin-dependent kinase II in the transition from pressure overload-induced cardiac hypertrophy to heart failure in mice. *J Clin Invest*. 2009;119:1230–1240. doi: 10.1172/JCI38022

28. Hegyi B, Borst JM, Bailey LRJ, Shen EY, Lucena AJ, Navedo MF, Bossuyt J, Bers DM. Hyperglycemia regulates cardiac K$^+$ channels via O-GlcNAc-CaMKII and NOX2-ROS-PKC pathways. *Basic Res Cardiol*. 2020;115:71. doi: 10.1007/s00395-020-00834-8

29. Clayton JA, Collins FS. Policy: NIH to balance sex in cell and animal studies. *Nature*. 2014;509:282–283. doi: 10.1038/509282a

30. Brunet S, Aimond F, Li H, Guo W, Eldstrom J, Fedida D, Yamada KA, Nerbonne JM. Heterogeneous expression of repolarizing, voltage-gated K$^+$ currents in adult mouse ventricles. *J Physiol*. 2004;559:103–120. doi: 10.1113/jphysiol.2004.063347

31. Brouillette J, Rivard K, Lizotte E, Fiset C. Sex and strain differences in adult mouse cardiac repolarization: importance of androgens. *Cardiovasc Res*. 2005;65:148–157. doi: 10.1016/j.cardiores.2004.09.012

32. Hegyi B, Fasoli A, Ko CY, Van BW, Alim CC, Shen EY, Ciccozzi MM, Tapa S, Ripplinger CM, Erickson JR, et al. CaMKII serine 280 O-GlcNAcylation links diabetic hyperglycemia to proarrhythmia. *Circ Res*. 2021;129:98–113. doi: 10.1161/CIRCRESAHA.120.318402

33. Brouillette J, Clark RB, Giles WR, Fiset C. Functional properties of K$^+$ currents in adult mouse ventricular myocytes. *J Physiol*. 2004;559:777–798. doi: 10.1113/jphysiol.2004.063446

34. Harikumar KB, Kunnumakkara AB, Ochi N, Tong Z, Deorukhkar A, Sung B, Kelland L, Jamieson S, Sutherland R, Raynham T, et al. A novel small-molecule inhibitor of protein kinase D blocks pancreatic cancer growth in vitro and in vivo. *Mol Cancer Ther*. 2010;9:1136–1146. doi: 10.1158/1535-7163.MCT-09-1145

35. Backs J, Backs T, Neef S, Kreusser MM, Lehmann LH, Patrick DM, Grueter CE, Qi X, Richardson JA, Hill JA, et al. The delta isoform of CaM kinase II is required for pathological cardiac hypertrophy and remodeling after pressure overload. *Proc Natl Acad Sci USA*. 2009;106:2342–2347. doi: 10.1073/pnas.0813013106

36. Kreusser MM, Lehmann LH, Keranov S, Hoting MO, Oehl U, Kohlhaas M, Reil JC, Neumann K, Schneider MD, Hill JA, et al. Cardiac CaM Kinase II genes delta and gamma contribute to adverse remodeling but redundantly inhibit calcineurin-induced myocardial hypertrophy. *Circulation*. 2014;130:1262–1273. doi: 10.1161/CIRCULATIONAHA.114.006185

37. Meredith EL, Ardayfio O, Beattie K, Dobler MR, Enyedy I, Gaul C, Hosagrahara V, Jewell C, Koch K, Lee W, et al. Identification of orally available naphthyridine protein kinase D inhibitors. *J Med Chem*. 2010;53:5400–5421. doi: 10.1021/jm100075z

38. Meredith EL, Beattie K, Burgis R, Capparelli M, Chapo J, Dipietro L, Gamber G, Enyedy I, Hood DB, Hosagrahara V, et al. Identification of potent and selective amidobipyridyl inhibitors of protein kinase D. *J Med Chem*. 2010;53:5422–5438. doi: 10.1021/jm100076w

39. Gilles P, Voets L, Van Lint J, De Borggraeve WM. Developments in the discovery and design of protein kinase D inhibitors. *ChemMedChem*. 2021;16:2158–2171. doi: 10.1002/cmdc.202100110

40. Wickenden AD, Kaprielian R, Kassiri Z, Tsoporis JN, Tsushima R, Fishman GI, Backx PH. The role of action potential prolongation and altered intracellular calcium handling in the pathogenesis of heart failure. *Cardiovasc Res*. 1998;37:312–323. doi: 10.1016/s0008-6363(97)00256-3

41. Wickenden AD, Lee P, Sah R, Huang Q, Fishman GI, Backx PH. Targeted expression of a dominant-negative K(v)4.2 K(+) channel subunit in the mouse heart. *Circ Res*. 1999;85:1067–1076. doi: 10.1161/01.res.85.11.1067

42. Helmstadter KG, Ljubojevic-Holzer S, Wood BM, Taheri KD, Sedej S, Erickson JR, Bossuyt J, Bers DM. CaMKII and PKA-dependent phosphorylation co-regulate nuclear localization of HDAC4 in adult cardiomyocytes. *Basic Res Cardiol*. 2021;116:11. doi: 10.1007/s00395-021-00850-2

43. He T, Huang J, Chen L, Han G, Stanmore D, Krebs-Haupenthal J, Avkiran M, Hagenmuller M, Backs J. Cyclic AMP represses pathological MEF2 activation by myocyte-specific hypo-phosphorylation of HDAC5. *J Mol Cell Cardiol*. 2020;145:88–98. doi: 10.1016/j.yjmcc.2020.05.018

44. Awad S, Al-Haffar KM, Marashly Q, Quijada P, Kunhi M, Al-Yacoub N, Wade FS, Mohammed SF, Al-Dayel F, Sutherland G, et al. Control of histone H3 phosphorylation by CaMKIIdelta in response to haemodynamic cardiac stress. *J Pathol*. 2015;235:606–618. doi: 10.1002/path.4489

45. Hegyi B, Bers DM, Bossuyt J. CaMKII signaling in heart diseases: emerging role in diabetic cardiomyopathy. *J Mol Cell Cardiol*. 2019;127:246–259. doi: 10.1016/j.yjmcc.2019.01.001

46. Wagner S, Hacker E, Grandi E, Weber SL, Dybkova N, Sossalla S, Sowa T, Fabritz L, Kirchhof P, Bers DM, et al. Ca/calmodulin kinase II differentially modulates potassium currents. *Circ Arrhythm Electrophysiol*. 2009;2:285–294. doi: 10.1161/CIRCEP.108.842799

47. Bers DM. Cardiac sarcoplasmic reticulum calcium leak: basis and roles in cardiac dysfunction. *Annu Rev Physiol*. 2014;76:107–127. doi: 10.1146/annurev-physiol-020911-153308

48. Ai X, Curran JW, Shannon TR, Bers DM, Pogwizd SM. Ca^{2+}/calmodulin-dependent protein kinase modulates cardiac ryanodine receptor phosphorylation and sarcoplasmic reticulum Ca^{2+} leak in heart failure. *Circ Res*. 2005;97:1314–1322. doi: 10.1161/01.RES.0000194329.41863.89

49. Wehrens XH, Lehnart SE, Reiken SR, Marks AR. Ca^{2+}/calmodulin-dependent protein kinase II phosphorylation regulates the cardiac ryanodine receptor. *Circ Res*. 2004;94:e61–e70. doi: 10.1161/01.RES.0000125626.33738.E2

50. van Oort RJ, McCauley MD, Dixit SS, Pereira L, Yang Y, Respress JL, Wang Q, De Almeida AC, Skapura DG, Anderson ME, et al. Ryanodine receptor phosphorylation by calcium/calmodulin-dependent protein kinase II promotes life-threatening ventricular arrhythmias in mice with heart failure. *Circulation*. 2010;122:2669–2679. doi: 10.1161/CIRCULATIONAHA.110.982298

51. Steffensen AB, Bomholtz SH, Andersen MN, Olsen JV, Mutsaers N, Lundegaard PR, Lundby A, Schmitt N. PKD phosphorylation as novel pathway to KV11.1 regulation. *Cell Physiol Biochem*. 2018;47:1742–1750. doi: 10.1159/000491007

52. Ozgen N, Obreztchikova M, Guo J, Elouardighi H, Dorn GW II, Wilson BA, Steinberg SF. Protein kinase D links Gq-coupled receptors to cAMP response element-binding protein (CREB)-Ser133 phosphorylation in the heart. *J Biol Chem*. 2008;283:17009–17019. doi: 10.1074/jbc.M709851200

53. Mason HS, Latten MJ, Godoy LD, Horowitz B, Kenyon JL. Modulation of Kv1.5 currents by protein kinase A, tyrosine kinase, and protein tyrosine phosphatase requires an intact cytoskeleton. *Mol Pharmacol*. 2002;61:285–293. doi: 10.1124/mol.61.2.285

54. Liljedahl M, Maeda Y, Colanzi A, Ayala I, Van Lint J, Malhotra V. Protein kinase D regulates the fission of cell surface destined transport carriers from the trans-Golgi network. *Cell*. 2001;104:409–420. doi: 10.1016/s0092-8674(01)00228-8

55. Nerbonne JM, Kass RS. Molecular physiology of cardiac repolarization. *Physiol Rev*. 2005;85:1205–1253. doi: 10.1152/physrev.00002.2005

56. Morotti S, Liu C, Hegyi B, Ni H, Fogli Iseppe A, Wang L, Pritoni M, Ripplinger CM, Bers DM, Edwards AG, et al. Quantitative cross-species translators of cardiac myocyte electrophysiology: model training, experimental validation, and applications. *Sci Adv*. 2021;7:eabg0927. doi: 10.1126/sciadv.abg0927

57. Hegyi B, Bossuyt J, Griffiths LG, Shimkunas R, Coulibaly Z, Jian Z, Grimsrud KN, Sondergaard CS, Ginsburg KS, Chiamvimonvat N, et al. Complex electrophysiological remodeling in postinfarction ischemic heart failure. *Proc Natl Acad Sci USA*. 2018;115:E3036–E3044. doi: 10.1073/pnas.1718211115

58. Hegyi B, Ko CY, Bossuyt J, Bers DM. Two-hit mechanism of cardiac arrhythmias in diabetic hyperglycaemia: reduced repolarization reserve, neurohormonal stimulation, and heart failure exacerbate susceptibility. *Cardiovasc Res*. 2021;117:2781–2793. doi: 10.1093/cvr/cvab006

59. Szentandrassy N, Kistamas K, Hegyi B, Horvath B, Ruzsnavszky F, Vaczi K, Magyar J, Banyasz T, Varro A, Nanasi PP. Contribution of ion

currents to beat-to-beat variability of action potential duration in canine ventricular myocytes. *Pflugers Arch.* 2015;467:1431–1443. doi: 10.1007/s00424-014-1581-4

60. Ronchi C, Badone B, Bernardi J, Zaza A. Action potential prolongation, beta-adrenergic stimulation, and angiotensin II as co-factors in sarcoplasmic reticulum instability. *Front Physiol.* 2018;9:1893. doi: 10.3389/fphys.2018.01893

61. Hegyi B, Polonen RP, Hellgren KT, Ko CY, Ginsburg KS, Bossuyt J, Mercola M, Bers DM. Cardiomyocyte Na⁺ and Ca²⁺ mishandling drives

vicious cycle involving CaMKII, ROS, and ryanodine receptors. *Basic Res Cardiol.* 2021;116:58. doi: 10.1007/s00395-021-00900-9

62. Weiss JN, Nivala M, Garfinkel A, Qu Z. Alternans and arrhythmias: from cell to heart. *Circ Res.* 2011;108:98–112. doi: 10.1161/CIRCRESAHA.110.223586

63. Jhun BS, O-Uchi J, Adaniya SM, Mancini TJ, Cao JL, King ME, Landi AK, Ma H, Shin M, Yang D, et al. Protein kinase D activation induces mitochondrial fragmentation and dysfunction in cardiomyocytes. *J Physiol.* 2018;596:827–855. doi: 10.1113/JP275418

SUPPLEMENTAL MATERIAL

Data S1.

SUPPLEMENTAL METHODS

Electrophysiology

Isolated left ventricular cardiomyocytes were transferred to a temperature-controlled chamber (Warner Instruments, Hamden, CT, USA) mounted on a Leica DMI3000B inverted microscope (Leica Microsystems, Buffalo Grove, IL, USA), and were continuously perfused (2 mL/min) with a bicarbonate-containing Tyrode solution having the following composition (in mmol/L): NaCl 124, $NaHCO_3$ 25, KCl 4, $CaCl_2$ 1.2, $MgCl_2$ 1, HEPES 10, glucose 10, with pH=7.4. The pH of bicarbonate-containing Tyrode's solution was regularly checked (every 2-hr) and carefully adjusted using a pH meter (VWR sympHony SB70P; VWR, Radnor, PA, USA). The osmolality of all applied solutions was also regularly checked and carefully adjusted to 295-300 mOsm/L using a vapor pressure osmometer (Vapro 5520; Wescor Inc., Logan, UT, USA). Action potentials (APs) and K^+ currents were recorded in whole-cell configuration of patch-clamp technique. Electrodes were fabricated from borosilicate glass (World Precision Instruments, Sarasota, FL, USA) having tip resistances of 2–2.5 MΩ when filled with internal solution containing (in mmol/L): K-Aspartate 100, KCl 20, NaCl 8, Mg-ATP 5, EGTA 10, $CaCl_2$ 4.1, HEPES 10, cAMP 0.002, phosphocreatine-K_2 10, and calmodulin 0.0001, with pH=7.2 (free $[Ca^{2+}]_i$=100 nmol/L, calculated using the WEBMAXC Extended version of the MaxChelator software, https://somapp.ucdmc.ucdavis.edu/pharmacology/bers/maxchelator/webmaxc/webmaxcE.htm). The electrodes were connected to the input of an Axopatch 200B amplifier (Axon Instruments, Union City, CA, USA). Outputs from the amplifier were digitized at 50 kHz using Digidata 1440A A/D card (Molecular Devices, San Jose, CA, USA) under software control (pClamp 10). The series resistance was typically 3–5 MΩ and it was compensated by 90%. Experiments were discarded when the series resistance was high or increased by >10%. Reported voltages are corrected to the liquid junction potentials. All experiments were conducted at 37±0.1°C.

APs were evoked by 2-ms-long supra-threshold depolarizing pulses delivered via the patch pipette at various pacing frequencies from 1 Hz to 10 Hz. Fifty consecutive APs were recorded and analyzed to examine the average behavior at each pacing frequency. Short-term variability of APD_{90} was calculated according to the following formula: $STV = \Sigma\,(\,|\,APD_{i+1} - APD_i\,|\,)\,/\,[(n_{beats} -1) * \sqrt{2}]$, where APD_i and APD_{i+1} indicate the durations of the ith and $(i+1)^{th}$ APs, and n_{beats} denotes the number of consecutive beats analyzed.[24,59] Changes in STV are presented as Poincaré plots, where 50 consecutive APD_{90} values are plotted, each against the duration of the previous APD_{90}. Experiments were performed when $[Ca^{2+}]_i$ was buffered to 100 nmol/L and also when EGTA and $CaCl_2$ were both omitted from the pipette solution listed above to preserve physiological $[Ca^{2+}]_i$ transient and contraction.

Whole-cell K^+ currents were recorded using 10 mmol/L EGTA (free $[Ca^{2+}]_i$=100 nmol/L) in the pipette solution, and in the presence of Na^+ and Ca^{2+} current inhibitors (10 µmol/L tetrodotoxin for I_{Na}, and 10 µmol/L nifedipine for I_{Ca}) in the bath solution. Different K^+ current components were separated using appropriate voltage protocols, selective ionic current inhibitors (5 mmol/L 4-aminopyridine for I_{to} and $I_{K,slow}$, 1 µmol/L E-4031 for I_{Kr}, 300 µmol/L $BaCl_2$ for I_{K1}) and biexponential fitting (R^2>0.9 in each case) to the decay of the voltage-gated outward K^+ currents (K_V) (Fig. S1) as previously described.[23,28,33] Voltage-gated K^+ currents (I_{Kv}) were elicited using a 4.5 s-long test pulses between -40 and +60 mV in 10 mV steps from a holding potential of -80 mV with an interpulse interval of 5.5 s.

For Ba^{2+}-sensitive I_{K1} traces, steady-state current–voltage relationships were obtained by plotting the magnitude of I_{K1} at the end of a 500-ms test pulse as a function of the test depolarization, arising from the holding potential of −80 mV. Ionic currents were normalized to cell capacitance (i.e., current density), determined in each cell using short (10 ms) hyperpolarizing pulses from −10 mV to −20 mV.

The impact of acute PKD inhibition was tested following 10 min cell treatment with the membrane-permeable, selective PKD inhibitor CRT0066101 (1 µmol/L) in self-controlled experiments.[34]

Diastolic arrhythmogenic activities were elicited by cessation of 1 min burst pacing (10 Hz), and membrane potential was recorded for an additional 3 min. Delayed afterdepolarizations (DADs) were defined as an increase in resting membrane potential exceeding 1 mV in amplitude within 0.5 s. Spontaneous APs (sAPs) were defined as depolarizations exceeding 0 mV (and having a fast upstroke

phase). The term of complex sAP was used when an early afterdepolarization (EAD) superimposed on sAP repolarization. EAD was defined as the inflexion of membrane potential change during repolarization, exceeding 3 mV in amplitude. DAD parameters were assessed only in those events where no AP occurred subsequently. DAD amplitude data were fitted to a log-normal distribution curve ($y = y_0 + A / (\sqrt{2\pi} * \omega x) * e^{\{-\ln[x/x_c]^2/2\omega^2\}}$), where y_0 is the offset, x_c is the center, ω is the log standard deviation and A is the area).

Data processing, analysis, and plotting have been performed using Clampfit 10 (Molecular Devices, San Jose, CA, USA), Excel for Office 365 (Microsoft, Redmond, WA, USA), GraphPad Prism 9 (GraphPad Software, San Diego, CA, USA) and Origin 2016 (OriginLab, Northampton, MA, USA) software.

Reagents
Chemicals and reagents were purchased from MilliporeSigma (St. Louis, MO, USA), if not specified otherwise. E-4031 was from Tocris (Bristol, UK).

Statistical analysis
Pooled data are presented as Mean±SEM. The number of biological and technical replicates in each experimental group is reported in the figures and figure legends. Normality of the data was assessed by Shapiro-Wilk test and the equality of group variance was tested using Brown-Forsythe test. Because multiple cells may come from one animal, we performed hierarchical statistical analysis taking into account inter-subject variability. Statistical significance of differences for continuous variables was tested by a linear-mixed model using nested ANOVA followed by a post hoc Tukey test, when applicable. Categorical outcomes were evaluated using Fisher's exact test. GraphPad Prism 9 (San Diego, CA, USA) software was used for data analysis. Blinded data acquisition and analysis have been performed for all *in vivo* experiments (echocardiography). Animals were grouped with no blinding but randomized in cellular experiments. Fully blinded analysis was not performed in cellular studies because the same person carried out the experiments and analysis. Both male and female animals were used. Group sizes were determined by an a priori power analysis for a two-tailed Student's *t*-test with an α of 0.05 and power of 0.8, in order to detect a 20% difference signal at the endpoint. Origin 2016 (OriginLab, Northampton, MA, USA) software was used for plotting the data.

	WT+Sham		PKD1 cKO+Sham		WT+TAC		PKD1 cKO+TAC	
Sex	Male	Female	Male	Female	Male	Female	Male	Female
N (animals)	4	4	4	3	8	8	7	6
EF pre-op (%)	53.1±5.0	52.1±4.6^{NS}	53.5±2.1	48.9±1.1^{NS}	56.5±3.5	59.1±4.7^{NS}	54.5±2.5	55.4±5.4^{NS}
EF 7 wks post-op (%)	53.3±4.6	55.5±6.5^{NS}	48.9±1.9	52.5±3.4^{NS}	26.6±2.9	27.4±3.0^{NS}	22.9±3.8	26.6±4.0^{NS}
Heart weight (HW, g)	0.25±0.01	0.21±0.01$^{P=0.02}$	0.25±0.02	0.22±0.02^{NS}	0.50±0.02	0.46±0.02^{NS}	0.41±0.05	0.31±0.04^{NS}
Body weight (BW, g)	32.7±1.2	25.2±1.6$^{P=0.01}$	30.9±1.0	28.2±0.5$^{P=0.07}$	29.1±0.6	25.5±0.7$^{P=0.01}$	28.5±1.0	23.6±1.2$^{P=0.01}$
HW / BW (%)	0.78±0.01	0.83±0.04^{NS}	0.79±0.04	0.77±0.08^{NS}	1.74±0.07	1.79±0.06^{NS}	1.43±0.18	1.32±0.08^{NS}
n (cells)	35	22	26	33	30	35	32	21
C_m (pF)	146.7±2.0	146.2±2.4^{NS}	144.4±1.8	146.2±1.6^{NS}	268.0±9.2	251.7±7.3^{NS}	219.0±6.0	220.5±8.0^{NS}
I_{K1} @ -140 mV (pA/pF)	-26.5±0.9	-26.7±1.1^{NS}	-27.2±0.8	-27.8±0.9^{NS}	-14.2±0.6	-14.0±0.7^{NS}	-19.2±0.8	-18.8±0.7^{NS}
I_{to} @ +60 mV (pA/pF)	19.3±3.6	17.0±1.2^{NS}	25.8±2.0	21.5±2.8^{NS}	9.6±1.7	9.0±1.3^{NS}	16.9±2.1	14.2±1.2^{NS}
$I_{K,slow}$ @ +60 mV (pA/pF)	9.7±0.7	8.2±1.0^{NS}	9.9±1.3	8.3±0.9^{NS}	5.9±0.9	4.9±0.8^{NS}	5.1±0.4	4.9±0.5^{NS}
I_{sus} @ +60 mV (pA/pF)	7.4±0.2	7.7±0.4^{NS}	7.8±0.6	8.3±0.4^{NS}	5.8±0.3	5.3±0.5^{NS}	6.7±0.4	7.2±0.6^{NS}
I_{Kr} @ +60 mV (pA/pF)	0.47±0.04	0.45±0.02^{NS}	0.48±0.06	0.46±0.04^{NS}	0.31±0.03	0.28±0.03^{NS}	0.39±0.04	0.43±0.06^{NS}
APD_{90} @ 1 Hz (ms)	40.2±1.7	43.3±3.5^{NS}	31.3±2.2	34.3±1.1^{NS}	71.1±5.9	67.5±6.5^{NS}	59.1±3.9	53.0±6.1^{NS}

Table S1. Sex-differences in morphometric data, contractility and electrophysiological parameters in mice.
Male-female comparisons were made in each experimental group. Male-female differences were determined in each group using unpaired Student's *t*-test and *P* values are reported after each value in females (*NS*, not significant). Parameters having significant difference from WT+Sham are shown in red for PKD1 cKO+Sham and in blue for WT+TAC. Magenta color denotes significant difference between PKD1cKO+TAC and WT+TAC. ANOVA with Tukey post hoc test.
(WT, wild-type; PKD1 cKO, protein kinase D1 cardiomyocyte-specific knockout; TAC, transverse aortic constriction; EF, ejection fraction; C_m, membrane capacitance; I_{K1}; inward rectifier K^+ current; I_{to}, transient outward K^+ current; $I_{K,slow}$, slowly inactivating K^+ current; I_{sus}, sustained current; I_{Kr}, rapid delayed rectifier K^+ current; APD_{90}, action potential duration at 90% of repolarization.)

Gene	Protein	I_K	Forward primer (5' to 3')	Reverse primer (5' to 3')
Gapdh	GAPDH	N/A	AACAGCAACTCCCACTCTTC	CCTGTTGCTGTAGCCGTATT
S18	18S rRNA	N/A	AAAGCAGACATCGACCTCAC	GTACTTCCCATCCTTCACATCC
Prkd1	PKD1	N/A	GCAGTGGAGTTAGAAGGAGAAG	GGCTCACAGGAGACAGTAAAG
Prkd2	PKD2	N/A	GGTATTCGTGGTGATGGAGAAA	CACCAGGATCTGCGTGATAAG
Prkd3	PKD3	N/A	GCATTTCACAAGGCAGTAACC	GGCAGCGAGAACAGGATTAT
Camk2d	CaMKIIδ	N/A	GTGACACCTGAAGCCAAAGA	CATCATGGAGGCAACAGTAGAG
Camk2f	CaMKIIγ	N/A	AAGCTGGAGCCTACGATTTC	GCGCTTTGCAGGGTTTATG
Nppa	ANF	N/A	CAGGCCATATTGGAGCAAATC	GGGCATGACCTCATCTTCTAC
Myh7	β-MHC	N/A	AGATGGCTGGTTTGGATGAG	TTGGCCTTGGTCAGAGTATTG
Hprt	HPRT	N/A	CTGATTATGGACAGGACTGAAAGA	AATCCAGCAGGTCAGCAAA
Kcnd2	$K_V4.2$	$I_{to,fast}$	CGCCACATCCTCAACTTCTA	CGGTCCTTGTACTCCTCATAAC
Kcnd3	$K_V4.3$	$I_{to,fast}$	GTGGCCATCATGCCCTATTA	GAAGATCCTGAAGACACGGAAG
Kcnip2	KChIP2	$I_{to,fast}$	TGATAGACTGAACTGGGCTTTC	GTAGGTGTACTTGCCCATCAT
Kcna4	$K_V1.4$	$I_{to,slow}$	ATCGTGGAGACAGTGTGTATTG	GCCCAGAGTGATGAAGTAAGG
Kcna5	$K_V1.5$	$I_{K,slow}$	TGAGGATGAGGAGGGAGAAG	CGCAAACCCGAGATGTTTATG
Kcnb1	$K_V2.1$	$I_{K,slow}$	GGCTTGTATCACGATCCTCTTAG	GCACTTGCTGTGGTGTAGAT
Kcnk2	TREK-1	I_{sus}	CTGTTTGGCTGTGTCCTCTT	CTGCCACGTAGTCTCCAAATC
Kcnk3	TASK-1	I_{sus}	GGACTTTCTTCCAGGCCTATT	GAAGCTGAAGGCCACATACT
Kcnj2	$K_{ir}2.1$	I_{K1}	GGTACCTGGCAGACATCTTTAC	GAGCAGGGCTATCAACCAAA
Kcnj12	$K_{ir}.2.2$	I_{K1}	AAGGGCCTAGACCGTATCTT	CTCAAAGTCGTCTGTCTCAAGG
Kcnh2a	hERG1a	I_{Kr}	CCCTCCATCAAGGACAAGTATG	GCATGACACAGATGGAGAAGA
Kcnh2b	hERG1b	I_{Kr}	GCTTACTGCCCTCTACTTCATC	CTTTCCAGGACGGGCATATAG

Table S2. Sequences of the specific primers used in RT-qPCR.
Examined genes, encoded proteins and related K^+ currents (I_K, if applicable) with the corresponding forward and reverse primers are listed.
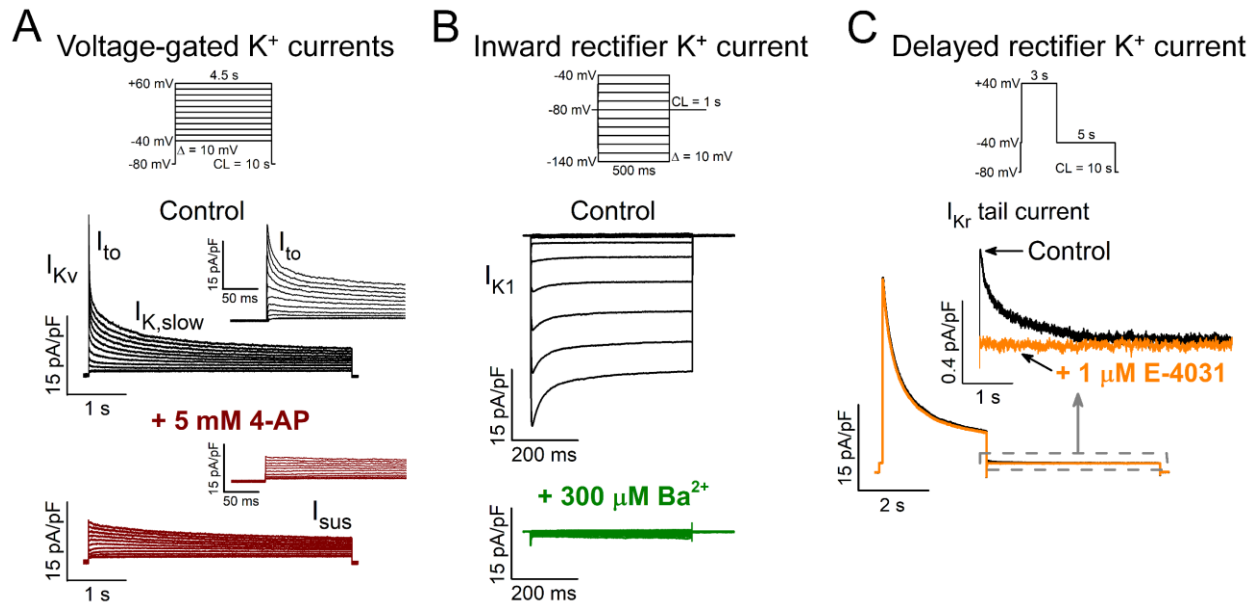
Figure S1. Major voltage-dependent K$^+$ currents in murine ventricular myocytes.
A, Representative voltage-gated outward K$^+$ current (I$_{Kv}$) traces in control and following 4-aminopyridine (4-AP, 5 mmol/L) treatment in mouse ventricular cardiomyocytes. 4-AP inhibits both the fast, transient outward K$^+$ current (I$_{to}$) and slowly inactivating K$^+$ current (I$_{K,slow}$), but not the sustained K$^+$ current (I$_{sus}$). Early phase of I$_{Kv}$ representing I$_{to}$ is enlarged in inset. I$_{to}$ and I$_{K,slow}$ were separated by biexponential fitting (R^2>0.9 in each case) to the decay of I$_{Kv}$. Sustained K$^+$ current (I$_{sus}$) was measured at the end of the 4.5s-long test voltage pulse. **B**, Representative inward rectifier K$^+$ current (I$_{K1}$) traces in control and following Ba^{2+} (300 µmol/L) treatment. I$_{K1}$ magnitude was measured at the end of a 500 ms test pulse. **C**, Representative rapid delayed rectifier K$^+$ current (I$_{Kr}$) traces in control and following E-4031 (1 µmol/L) treatment. I$_{Kr}$ tail current is enlarged in inset. The tail current was completely inhibited by E-4031 treatment. Whole-cell K$^+$ currents were recorded using 10 mmol/L EGTA (free [Ca^{2+}]$_i$=100 nmol/L) in the pipette solution, and in the presence of Na$^+$ and Ca^{2+} channel inhibitors (10 µmol/L tetrodotoxin for voltage-gated Na$^+$ channel, and 10 µmol/L nifedipine for L-type Ca^{2+} channel) in the external Tyrode's solution. Voltage protocols are shown above (CL, cycle length).
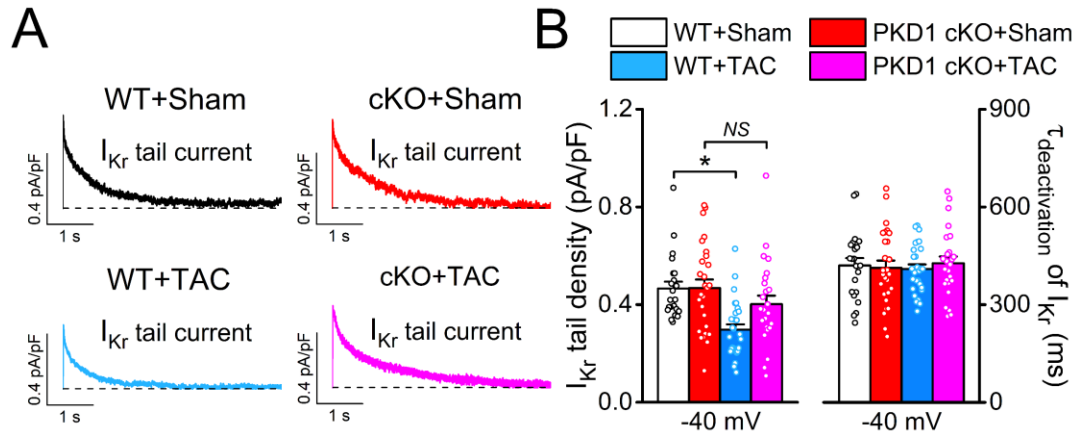
Figure S2. Rapid delayed rectifier K$^+$ current in murine ventricular myocytes.
A, Representative rapid delayed rectifier K$^+$ current (I_{Kr}) tails. **B**, I_{Kr} tail density and deactivation time constant. (Number of animals, WT+Sham: 8, PKD1 cKO+Sham: 5, WT+TAC: 6, and PKD1 cKO+TAC: 5. The number of cells (n) in each experimental group is listed in the figure.) Nested ANOVA with Tukey post hoc test. *P<0.05 versus WT+Sham.
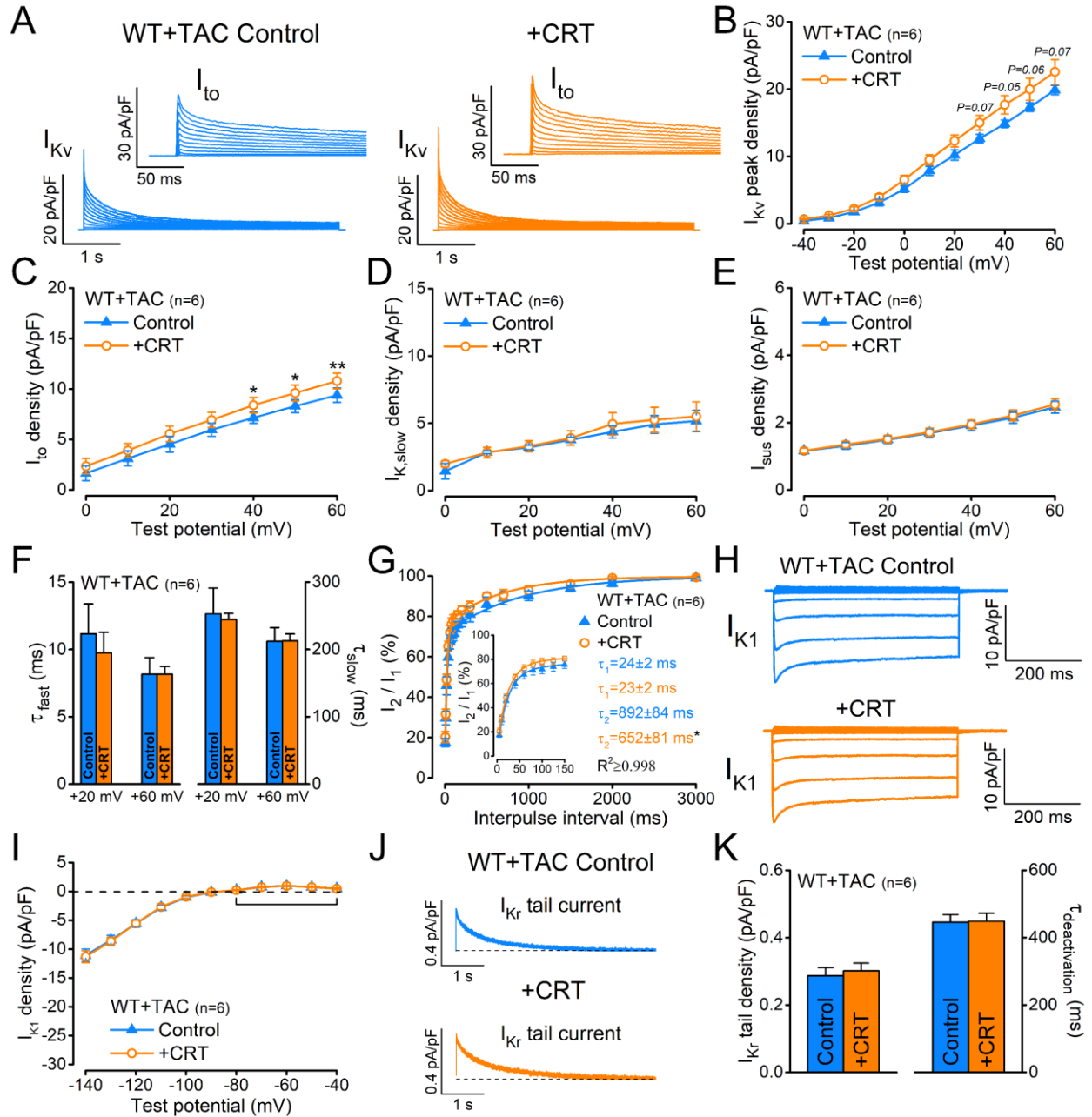
Figure S3. Effect of acute PKD inhibition on K⁺ currents in TAC-induced HF.

A, Representative voltage-gated outward K^+ current (I_{Kv}) traces in wild-type (WT) ventricular cardiomyocytes 8-wk post-TAC in control and following 10-min treatment with the selective PKD inhibitor, CRT0066101 (CRT, 1 μmol/L). Early phase of I_{Kv} is enlarged in inset. **B**, Peak I_{Kv} density. **C**, Transient outward K^+ current (I_{to}) density. **D**, Slowly inactivating K^+ current ($I_{K,slow}$) density. **E**, Sustained K^+ current (I_{sus}) density. **F**, I_{to} inactivation time constants (τ_{fast} and τ_{slow}). **G**, I_{to} recovery from inactivation. Rapid recovery shown in inset. **H**, Representative inward rectifier K^+ current (I_{K1}) traces. **I**, I_{K1} density-voltage relationship. Outward I_{K1} is enlarged in inset. **J**, Representative rapid delayed rectifier K^+ current (I_{Kr}) tails. **K**, I_{Kr} tail density and deactivation time constant. (n=6 cells/3 animals in each experimental group). Paired, two-tailed Student's t-test. *$P<0.05$, **$P<0.01$.
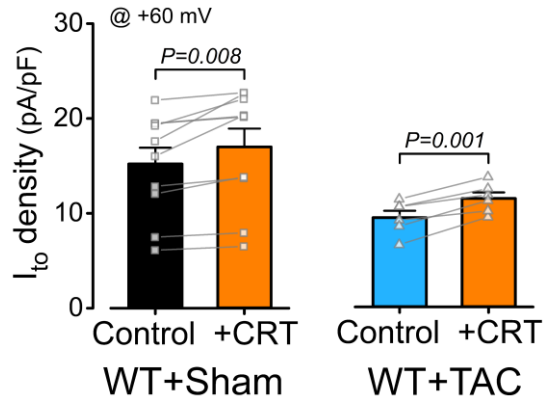
Figure S4. Acute PKD inhibition enhances the transient outward K$^+$ current (I$_{to}$).
Acute inhibition of PKD using the selective inhibitor CRT0066101 (CRT, 1 μmol/L, 10 min) increased the density of the transient outward K$^+$ current (I$_{to}$) in wild-type (WT) sham (n=10 cells/4 animals) and TAC (n=6 cells/3 animals) ventricular cardiomyocytes. I$_{to}$ density at +60 mV is shown in paired experiments before and after CRT treatment. Paired, two-tailed Student's t-test.
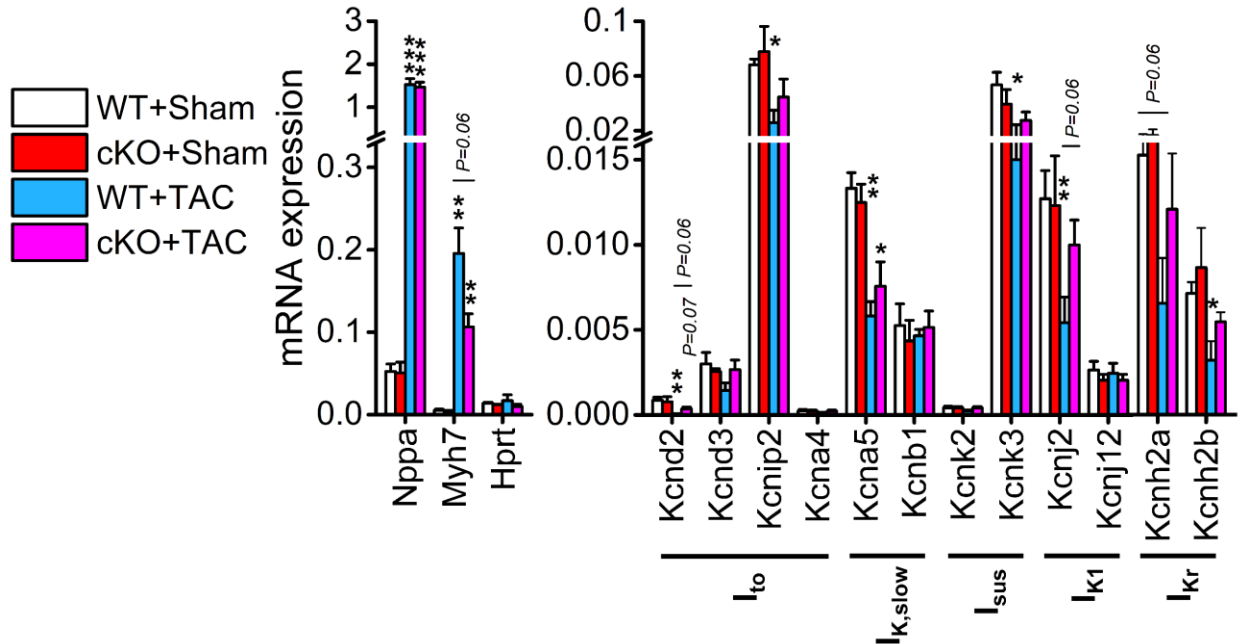
Figure S5. Expression of K⁺ channels in WT and PKD1 cKO mouse hearts.
Expression of hypertrophic genes (atrial natriuretic peptide, Nppa; β-myosin heavy chain, Myh7) and K⁺ channel subunits in wild-type (WT) and PKD1 cardiac-specific knockout (cKO) ventricular cardiomyocytes 8-wk after TAC or sham. N=3 hearts in each experimental group, and 3 technical replicates have been performed and averaged for each heart. ANOVA with Bonferroni post hoc test. *P<0.05, **P<0.01, ***P<0.001 vs. WT Sham.
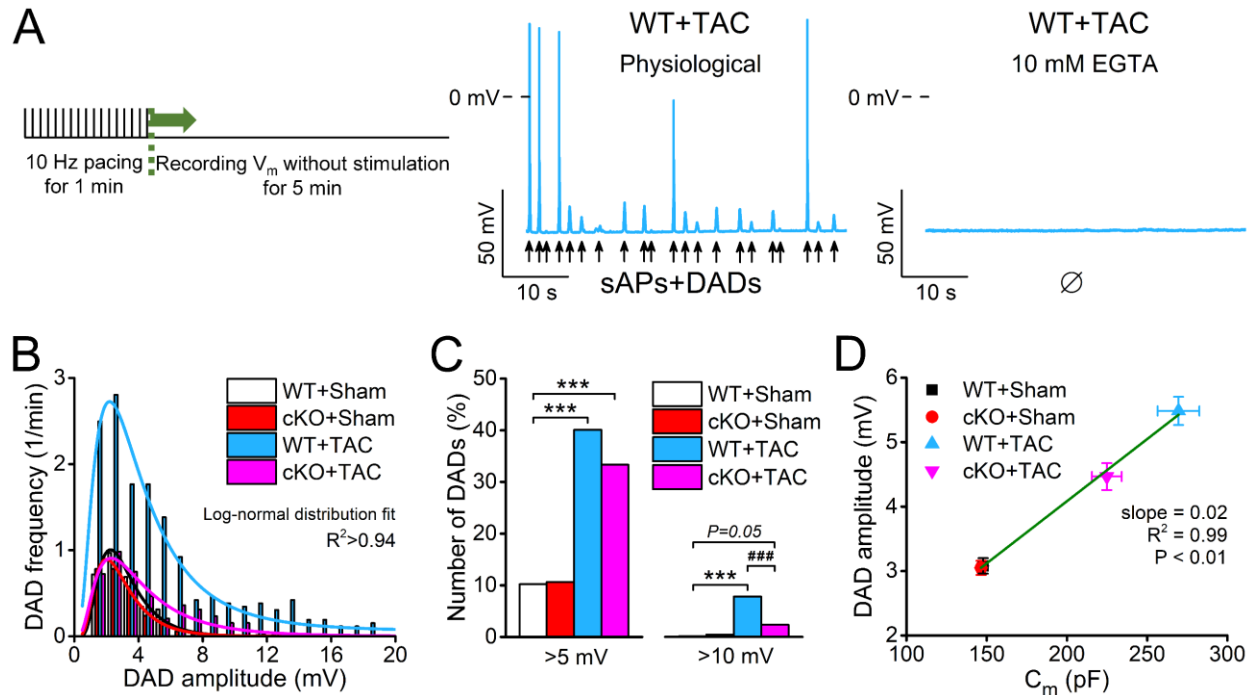
Figure S6. Delayed afterdepolarizations (DADs) in TAC-induced HF.
A, Arrhythmogenic diastolic activities were elicited using a tachypacing protocol (*left*). Representative records in isolated left ventricular WT cardiomyocytes 8-wk post-TAC under physiological conditions (without using exogenous Ca^{2+} buffers, *middle*) and in the presence of 10 mmol/L EGTA in the pipette solution ($[Ca^{2+}]_i$=100 nM, *right*). **B**, Correlation between DAD frequency and DAD amplitude in wild-type (WT) and PKD1 cKO ventricular cardiomyocytes 8-wk after TAC (or sham). DADs were measured following cessation of 1-min tachypacing at 10 Hz frequency. DAD amplitude data were fitted to a log-normal distribution curve (R^2>0.94 in all cases). **C**, Percentage of total DADs having amplitude of >5 mV and >10 mV. Fisher's exact test. ****P*<0.001 versus WT+Sham; ^###*P*<0.001 versus WT+TAC. **D**, Correlation between DAD amplitude and membrane capacitance in each experimental group measured. Solid line represents the linear fit to the data (R^2=0.99).